



Techniques of Water-Resources Investigations
of the United States Geological Survey

Chapter C3

**A MODEL FOR SIMULATION OF
FLOW IN SINGULAR AND
INTERCONNECTED CHANNELS**

By R. W. Schaffranek, R. A. Baltzer, and D. E. Goldberg

Book 7

AUTOMATED DATA PROCESSING AND COMPUTATIONS

UNITED STATES DEPARTMENT OF THE INTERIOR

JAMES G. WATT, Secretary

GEOLOGICAL SURVEY

Doyle G. Frederick, Acting Director

UNITED STATES GOVERNMENT PRINTING OFFICE, WASHINGTON : 1981

For sale by the Superintendent of Documents, U.S. Government Printing Office
Washington D.C. 20402

PREFACE

The series of manuals on techniques describes procedures for planning and executing specialized work in water-resources investigations. The material is grouped under major headings called books and further subdivided into sections and chapters; section C of Book 7 is on computer programs.

This chapter presents a digital computer model for simulating the unsteady flow regimen occurring in a singular reach or throughout a system of reaches composed of simply or multiply connected one-dimensional-flow channels governed by time-dependent forcing functions and boundary conditions. The model is broadly applicable to a wide range of hydrologic conditions and field situations. Channel geometry need not be prismatic. Reach lengths of the branches and segments used in the model need not be equal. Procedures to be followed in implementing the model to a specific field application are presented in a straightforward, step-by-step manner. Operational modeling capability is achieved by linking the model to a highly efficient storage-and-retrieval routine that accesses a data base containing time series of boundary values. This operational capability is enhanced by optional linkage to an extensive set of digital graphics subroutines. Although the model is well tested and will efficiently produce reliable flow computations for a wide variety of field applications, the user is reminded that achieving successful simulation modeling is not dependent solely on employing a well-formulated model. The user's knowledge and understanding of hydrodynamic principles, his willingness to recognize and abide by the limitations inherent in the model, his imagination and skill—seasoned by experience—in schematizing the prototype for modeling, and his common-sense ability to recognize errant data or results are important attributes, all contributing to successful simulation modeling.

Any use of trade names and trademarks in this publication is for descriptive purposes only and does not constitute endorsement by the U S Geological Survey

TECHNIQUES OF WATER-RESOURCES INVESTIGATIONS OF THE U.S. GEOLOGICAL SURVEY

The U.S. Geological Survey publishes a series of manuals describing procedures for planning and conducting specialized work in water-resources investigations. The manuals published to date are listed below and may be ordered by mail from the **Branch of Distribution, U.S. Geological Survey, 1200 South Eads Street, Arlington, VA 22202** (an authorized agent of the Superintendent of Documents, Government Printing Office).

Prepayment is required. Remittances should be sent by check or money order payable to U.S. Geological Survey. Prices are not included in the listing below as they are subject to change. **Current prices can be obtained by calling the USGS Branch of Distribution, phone (202) 751-6777.** Prices include cost of domestic surface transportation. For transmittal outside the U.S.A. (except to Canada and Mexico) a surcharge of 25 percent of the net bill should be included to cover surface transportation.

When ordering any of these publications, please give the title, book number, chapter number, and "U.S. Geological Survey Techniques of Water-Resources Investigations."

- TWI 1-D1. Water temperature—influential factors, field measurement, and data presentation, by H. H. Stevens, Jr., J. F. Ficke, and G. F. Smoot. 1975. 65 pages.
- TWI 1-D2. Guidelines for collection and field analysis of ground-water samples for selected unstable constituents, by W. W. Wood. 1976. 24 pages.
- TWI 2-D1. Application of surface geophysics to ground-water investigations, by A. A. R. Zohdy, G. P. Eaton, and D. R. Mabey. 1974. 116 pages.
- TWI 2-E1. Application of borehole geophysics to water-resources investigations, by W. S. Keys and L. M. MacCary. 1971. 126 pages.
- TWI 3-A1. General field and office procedures for indirect discharge measurements, by M. A. Benson and Tate Dalrymple. 1967. 30 pages.
- TWI 3-A2. Measurement of peak discharge by the slope-area method, by Tate Dalrymple and M. A. Benson. 1967. 12 pages.
- TWI 3-A3. Measurement of peak discharge at culverts by indirect methods, by G. L. Bodhaine. 1968. 60 pages.
- TWI 3-A4. Measurement of peak discharge at width contractions by indirect methods, by H. F. Matthai. 1967. 44 pages.
- TWI 3-A5. Measurement of peak discharge at dams by indirect methods, by Harry Hulsing. 1967. 29 pages.
- TWI 3-A6. General procedure for gaging streams, by R. W. Carter and Jacob Davidian. 1968. 13 pages.
- TWI 3-A7. Stage measurements at gaging stations, by T. J. Buchanan and W. P. Somers. 1968. 28 pages.
- TWI 3-A8. Discharge measurements at gaging stations, by T. J. Buchanan and W. P. Somers. 1969. 65 pages.
- TWI 3-A11. Measurement of discharge by moving-boat method, by G. F. Smoot and C. E. Novak. 1969. 22 pages.
- TWI 3-B1. Aquifer-test design, observation, and data analysis, by R. W. Stallman. 1971. 26 pages.
- TWI 3-B2. Introduction to ground-water hydraulics, a programed text for self-instruction, by G. D. Bennett. 1976. 172 pages.
- TWI 3-B3. Type curves for selected problems of flow to wells in confined aquifers, by J. E. Reed.
- TWI 3-C1. Fluvial sediment concepts, by H. P. Guy. 1970. 55 pages.
- TWI 3-C2. Field methods for measurement of fluvial sediment, by H. P. Guy and V. W. Norman. 1970. 59 pages.

- TWI 3-C3. Computation of fluvial-sediment discharge, by George Porterfield. 1972. 66 pages.
- TWI 4-A1. Some statistical tools in hydrology, by H. C. Riggs. 1968. 39 pages.
- TWI 4-A2. Frequency curves, by H. C. Riggs. 1968. 15 pages.
- TWI 4-B1. Low-flow investigations, by H. C. Riggs. 1972. 18 pages.
- TWI 4-B2. Storage analyses for water supply, by H. C. Riggs and C. H. Hardison. 1973. 20 pages.
- TWI 4-B3. Regional analyses of streamflow characteristics, by H. C. Riggs. 1973. 15 pages.
- TWI 4-D1. Computation of rate and volume of stream depletion by wells, by C. T. Jenkins. 1970. 17 pages.
- TWI 5-A1. Methods for determination of inorganic substances in water and fluvial sediments, by M. W. Skougstad and others, editors. 1979. 626 pages.
- TWI 5-A2. Determination of minor elements in water by emission spectroscopy, by P. R. Barnett and E. C. Mallory, Jr. 1971. 31 pages.
- TWI 5-A3. Methods for analysis of organic substances in water, by D. F. Goerlitz and Eugene Brown. 1972. 40 pages.
- TWI 5-A4. Methods for collection and analysis of aquatic biological and microbiological samples, edited by P. E. Greeson, T. A. Ehlke, G. A. Irwin, B. W. Lum, and K. V. Slack. 1977. 332 pages.
- TWI 5-A5. Methods for determination of radioactive substances in water and fluvial sediments, by L. L. Thatcher, V. J. Janzer, and K. W. Edwards. 1977. 95 pages.
- TWI 5-C1. Laboratory theory and methods for sediment analysis, by H. P. Guy. 1969. 58 pages.
- TWI 7-C1. Finite difference model for aquifer simulation in two dimensions with results of numerical experiments, by P. C. Trescott, G. F. Pinder, and S. P. Larson. 1976. 116 pages.
- TWI 7-C2. Computer model of two-dimensional solute transport and dispersion in ground water, by L. F. Konikow and J. D. Bredehoeft. 1978. 90 pages.
- TWI 7-C3. A model for simulation of flow in singular and interconnected channels, by R. W. Schaffranek, R. A. Baltzer, and D. E. Goldberg.
- TWI 8-A1. Methods of measuring water levels in deep wells, by M. S. Garber and F. C. Koopman. 1968. 23 pages.
- TWI 8-B2. Calibration and maintenance of vertical-axis type current meters, by G. F. Smoot and C. E. Novak. 1968. 15 pages.

CONTENTS

	Page		Page
Symbols and units	IX	Branch-network program description—Continued	
Abstract	1	Model application	26
Introduction	1	Program run preparation	28
Acknowledgments	3	Data input	28
Unsteady-flow equations for networks of open		Job control	30
channels	3	Program versions	32
Flow equations	3	Storage and time requirements	32
Boundary conditions	5	Diagnostic messages	33
Compatibility conditions at internal junctions	5	Input/output description	35
Boundary conditions at external junctions	5	Branch-network model applications	40
Initial conditions	6	Sacramento-Freeport reach of the Sacramento	
Solution technique for open-channel network flow		River	42
simulation	6	Columbia River reach at Rocky Reach Dam near	
Finite-difference formulation	6	Wenatchee, Wash	43
Coefficient-matrix formulation	8	Kootenai River reach near Porthill, Idaho	45
Branch-transformation equation	8	Connecticut River reach near Hartford, Conn	49
Matrix solution	9	Detroit River between Lake St. Clair and Lake	
Branch-network model implementation	11	Eric	49
Channel and cross-sectional geometry	11	Summary	58
Channel conveyance parameters	12	References cited	58
Initial and boundary-value data	14	Appendix I, Program control-card format	63
Computation-control parameters	15	Appendix II, Definition of MAIN program variables	
Calibration and verification	18	and arrays	67
Branch-network program description	25	Appendix III, Adjustable arrays	72
Program restrictions	26	Appendix IV, FORTRAN IV program listing	73

FIGURES

	Page
1. Definition schematic of a hypothetical network	3
2. Definition sketch of a channel cross section	4
3, 4. Diagrams of:	
3. Space-time-grid system for finite-difference approximations	6
4. A simple hypothetical network	10
5. Coefficient matrices for the hypothetical network shown in figure 4	10
6-14. Graphs of:	
6. Discharges computed for the Sacramento River near Freeport, Calif., by use of various initial values in the branch-network flow model	14
7. Discharges computed for the Sacramento River near Freeport, Calif., by use of various time increments in the branch-network flow model	16
8. Water-surface elevations for the Sacramento River at Sacramento, Calif., and near Freeport, Calif., used as boundary-value data for the branch-network flow-model simulation shown in figure 7	17
9. Steady-flow computations for the Sacramento River at Sacramento, Calif., by use of various finite-difference weighting factors (θ) in the branch-network flow model	18
10. Discharges computed for the Sacramento River at Sacramento, Calif., with flow resistance increased and decreased by 25 percent	21

	Page
6-14. Graphs of Continued	
11. Discharges computed for the Sacramento River at Sacramento, Calif., with the fall increased and decreased by 1.52 centimeters	22
12. Discharges computed for the Sacramento River at Sacramento, Calif., with the cross-sectional area and top width increased and decreased by 10 percent	23
13. Discharges computed for the Sacramento River at Sacramento, Calif., with various weighting factors (θ) for the spatial derivatives in the branch-network flow model	24
14. Discharges computed for the Sacramento River at Sacramento, Calif., with various weighting factors (χ) for the function values in the branch-network flow model	24
15. Diagram showing the input-card order for the branch-network flow model	29
16-18. Listings of:	
16. FORTRAN IV code used to negate the DISSPLA coded plot subroutine, OPLOT, from the branch-network flow model	32
17. FORTRAN IV code used to negate the time-dependent boundary-value-data storage-and-retrieval subroutine, DADIO, from the branch-network flow model	33
18. Sample deck setup to execute the branch-network flow model of the Sacramento-Freeport reach of the Sacramento River	36
19. Sample output from the simulation-deck setup of Figure 18, with IOTOPT option 3 and IPLOPT option 3.	
A. List of control card parameters assigned by card or default. B. Branch-identification parameters, cross-sectional geometry tables, and initial values. C. Desired line-printer plot of computed versus measured discharge for the Sacramento River at Sacramento, Calif	37
20. Computed flow results at each time step printed in tabular form, produced using IOTOPT option 0	38
21. Sample printout of monthly accumulated flow-volume summary, produced using IOTOPT option 4	39
22. Listing of TSO allocation and execution commands for Tektronix plotting by use of the DISSPLA Post Processor	40
23. Photograph showing a closeup view of Tektronix cathode-ray-tube display unit	41
24. Map of the Sacramento River reach near Sacramento, Calif	43
25. Model-generated plot of computed-versus-measured discharges for the Sacramento River, produced using IOTOPT option 3, IPLOPT option 3, and IPLDEV option 2	44
26. Map of the Columbia River reach near Rocky Reach Dam in the State of Washington	45
27. Model-generated plot of computed discharges for the Columbia River, produced using IOTOPT option 3, IPLOPT option 1, and IPLDEV option 2	46
28. Map of the Kootenai River reach near Porthill, Idaho	47
29. Sample output of the daily summary of computed flow for the Kootenai River produced using IOTOPT option 2	48
30. Map of the Connecticut River reach near Hartford, Conn	50
31. Model-generated plot of computed-versus-measured water-surface elevations for the Connecticut River, produced using IOTOPT option 3, IPLOPT option 4, and IPLDEV option 2	51
32. Model-generated hydrographs of computed discharges for the Connecticut River, branches 1 and 2, produced using IOTOPT option 3, IPLOPT option 1, and IPLDEV option 2	52
33. Map of the Detroit River near Detroit, Mich	54
34. Diagram of the schematization of the Detroit River for the branch-network flow model	55
35. Listing of a sample deck setup to execute the branch-network flow model of the Detroit River	56
36. Model-generated plot of computed-versus-measured water-surface elevations for the Detroit River, produced using IOTOPT option 3, IPLOPT option 4, and IPLDEV option 2	57

TABLES

	Page
International System of Units (SI) and inch-pound equivalents	IX
1. Stage-area-width relationships for the Sacramento River at Sacramento, Calif	28
2. Symbolic parameters of the BRANCH cataloged procedure	31
3. Composite list of output examples and appropriate values of the output-control variables	38

INTERNATIONAL SYSTEM OF UNITS (SI) AND INCH-POUND SYSTEM EQUIVALENTS

SI unit	Inch-pound equivalent
Length	
centimeter (cm) =	0.3937 inch (in)
meter (m) =	3.281 feet (ft)
kilometer (km) =	0.6214 mile (mi)
Area	
centimeter ² (cm ²) =	0.1550 inch ² (in ²)
meter ² (m ²) =	10.76 feet ² (ft ²)
kilometer ² (km ²) =	0.3861 mile ² (mi ²)
Volume	
centimeter ³ (cm ³) =	0.06102 inch ³ (in ³)
meter ³ (m ³) =	35.31 feet ³ (ft ³)
	= 8.107 × 10 ⁻⁴ acre-foot (acre-ft)
Volume per unit time	
meter ³ per second (m ³ /s) =	35.31 feet ³ per second (ft ³ /s)
	= 1.585 × 10 ⁴ gallons per minute (gal/min)
Mass per unit volume	
kilogram per meter ³ (kg/m ³) =	0.06243 pound per foot ³ (lb/ft ³)
gram per centimeter ³ (g/cm ³) =	6.243 × 10 ⁻⁵ pound per foot ³ (lb/ft ³)
Temperature	
degree Celsius (°C) =	(degree Fahrenheit - 32)/1.8 (°F)

SYMBOLS AND UNITS

<i>Symbol</i>	<i>Definition</i>	<i>Unit</i>
<i>A</i>	cross-sectional area	L ²
<i>A</i>	coefficient matrix	
<i>B</i>	channel top width	L
<i>B</i>	vector of constants	
<i>c</i>	wave celerity (\sqrt{gH})	LT ⁻¹
<i>C_d</i>	water-surface drag coefficient	
<i>dA</i>	a finite elemental area	L ²
<i>f</i>	a function	
<i>f(I)</i>	functional representation of a dependent variable	
<i>g</i>	acceleration of gravity	LT ⁻²
<i>H</i>	hydraulic depth (<i>A/B</i>)	L
<i>i</i>	subscript index which denotes a function's spatial location	
<i>j</i>	superscript index which denotes a function's temporal location	
<i>k</i>	function of the flow-resistance coefficient $\left(\frac{\eta}{1.49}\right)^2$ in inch-pound system; η^2 in metric system)	T ² L ^{-2/3}
<i>K</i>	channel conveyance $\left(\frac{1}{\sqrt{k}} AR^{2/3}\right)$	L ³ T ⁻¹
<i>n</i>	Manning's flow-resistance coefficient	TL ^{-1/3}
<i>Q</i>	flow discharge	L ³ T ⁻¹

<i>Symbol</i>	<i>Definition</i>	<i>Unit</i>
Q_1^I, \dots, Q_4^{III}	elements of the vector of unknowns, \mathbf{X} , representing the flow discharge of a branch (I,II,III) at a junction (1,2,3,4)	L^3T^{-1}
Q_m	flow discharge of m th branch at a junction	L^3T^{-1}
R	hydraulic radius of cross section	L
S	slope of energy line	
\mathbf{S}	vector of state	
t	time	T
Δt	time increment	T
u	flow velocity at a point	LT^{-1}
\mathbf{u}	transformation matrix	
u_1^I, \dots, u_2^{III}	elements of the vector of constants, \mathbf{B} , which define, in part, the branch-transformation equation of a branch (I,II,III)	
$\mathbf{u}_{(i)}$	transformation matrix of i th segment	
\mathbf{u}_n	transformation matrix of n th branch	
U	mean velocity in cross section	LT^{-1}
\mathbf{U}	transformation matrix	
$U_{11}^I, \dots, U_{22}^{III}$	elements of the coefficient matrix, \mathbf{A} which define, in part, the branch-transformation equation of a branch (I,II,III)	
$\mathbf{U}_{(i)}$	transformation matrix of i th segment	
\mathbf{U}_n	transformation matrix of n th branch	
U_a	wind velocity	LT^{-1}
W	nodal flow	L^3T^{-1}
W_k	nodal flow at k th junction	L^3T^{-1}
x	longitudinal distance along channel	L
Δx	length	L
Δx_i	length of i th segment	L
\mathbf{X}	vector of unknowns	
$z_1(t), \dots, z_4(t)$	elements of the vector of constants, \mathbf{B} , representing the time-dependent water-surface elevation at a junction (1,2,3,4)	L
Z	water-surface elevation	L
Z_1^I, \dots, Z_4^{III}	elements of the vector of unknowns, \mathbf{X} , representing the water-surface elevation of a branch (I,II,III) at a junction (1,2,3,4)	L
Z_m	water-surface elevation of m th branch at a junction	L
α	angle between wind direction and x -axis	(deg)
β	momentum coefficient	
γ	flow-equation coefficient	
δ	flow-equation coefficient	
ϵ	flow-equation coefficient	
ζ	flow-equation coefficient	
η	flow-resistance coefficient similar to Manning's n	$TL^{-1/3}$
θ	spatial-derivative weighting factor	
λ	flow-equation coefficient	
μ	flow-equation coefficient	
ξ	wind-resistance coefficient $\left(C_d \frac{\rho_a}{\rho}\right)$	
ρ	water density	ML^{-3}
ρ_a	atmospheric density	ML^{-3}
σ	flow-equation coefficient	
χ	weighting factor for function values	
ω	flow-equation coefficient	
\sim	superscript notation used to signify function values derived from the previous iteration	

A MODEL FOR SIMULATION OF FLOW IN SINGULAR AND INTERCONNECTED CHANNELS

By R. W. Schaffranek, R. A. Baltzer, and D. E. Goldberg

Abstract

A one-dimensional numerical model is presented for simulating the unsteady flow in singular riverine or estuarine reaches and in networks of reaches composed of interconnected channels. The model is both general and flexible in that it can be used to simulate a wide range of flow conditions for various channel configurations. The channel geometry of the network to be modeled should be sufficiently simple so as to lend itself to characterization in one spatial dimension. The flow must be substantially homogenous in density, and hydrostatic pressure must prevail everywhere in the network channels. The slope of each channel bottom ought to be mild and reasonably constant over its length so that the flow remains subcritical. The model accommodates tributary inflows and diversions and includes the effects of wind shear on the water surface as a forcing function in the flow equations. Water-surface elevations and flow discharges are computed at channel junctions, as well as at specified intermediate locations within the network channels.

The one-dimensional branch-network flow model uses a four-point, implicit, finite-difference approximation of the unsteady-flow equations. The flow equations are linearized over a time step, and branch transformations are formulated that describe the relationship between the unknowns at the end points of the channels. The resultant matrix of branch-transformation equations and required boundary-condition equations is solved by Gaussian elimination using maximum pivot strategy.

Five example applications of the flow model are illustrated. The applications cover such diverse conditions as a singular upland river reach in which unsteady flow results from hydropower regulations, coastal rivers composed of sequentially connected reaches subject to unsteady tide-driven flow, and a multiply connected network of channels whose flow is principally governed by wind tides and seiches in adjoining lakes.

The report includes a listing of the FORTRAN IV computer program and a description of the input data requirements. Model supporting programs for the processing and input of initial and boundary-value data are identified, various model output formats are illustrated, and instructions are given to permit the production of graphical output using the line printer, electromechanical pen plotters, cathode-ray-tube display units, or microfilm recorders.

Introduction

Advent of efficient, economical electronic computation during the past two decades has had a profound effect on our means for conducting water-resources assessments. The two principal disciplines underpinning water-resources science—theoretical hydromechanics and experimental hydraulics—have been joined by the new and still emerging discipline of *computational hydromechanics*. This new discipline, while lying essentially at the intersection of theoretical hydromechanics, numerical analysis, and computer science and drawing upon the developmental progress in each of the others, is being recognized as an independent branch of knowledge in its own right. It makes use of the parametric information derived from hydraulic experimentation as well. In effect, computational hydromechanics is providing the means for transforming the theoretical knowledge of hydromechanics into useful and practical tools for water-resources study. The numerical model presented in this report is an example of just such a tool.

Research of flow simulation modeling in riverine and estuarine systems began in the U.S. Geological Survey in the late 1950's. The objective was to provide a strong physical basis for the development of methods with which to determine unsteady flows in channels affected by tides, flood waves, or hydropower regulation or where flow inertial effects were appreciable. Various numerical methods for treating the complete Saint Venant wave-propagation equations were studied, and various models were constructed and reported in the literature (Baltzer and Shen, 1961; Lai, 1965a, b). The

earliest models were designed to treat only a single reach of channel since the numerical methods were primitive and the computational capabilities of the day rather limiting. Models capable of representing systems composed of two or more sequentially connected reaches (Baltzer and Lai, 1968) were quickly followed by models capable of depicting dendritic channel systems comprising many connected subreaches. However, these early models lacked the support of a comprehensive modeling system with which to easily effect their implementation and a computer data base with which to broaden the scope of their use. Consequently, each new model implementation was done in an ad hoc manner. In the early 1970's work was begun on a general purpose computerized system, including a boundary-value data base and other supportive files, designed specifically for modular use in simulation modeling. Use of this comprehensive modeling system in conjunction with the branch-network flow model—the name given to the numerical simulation model described in this report—is demonstrated subsequently. Whether or not to use the model with the supportive modeling system is optional.

The branch-network flow model is based upon the one-dimensional, nonlinear partial-differential equations governing unsteady flow in channels for which the dependent variables are the flow rate, Q , and the water-surface elevation, Z . The application of the model is subject to the basic assumptions and limitations inherent in the equations' formulation as described in the report. The equations include terms accommodating the shear-stress effect of wind on the water surface and the Boussinesq momentum-correction coefficient permitting adjustment for nonuniformity of flow in the channel cross section. The partial-differential equations are discretized and replaced by the appropriate finite-difference equations according to a weighted, four-point scheme. Weighting factors governing the discretized quantities of functional values and space derivatives in the finite-difference equations are specifiable, thus providing the model user the flexibility to vary the implicit-solution technique from a box-centered scheme on the one hand to a fully forward scheme on the other. The model is unconditionally linearly stable throughout this range.

The branch-network flow model, as described and documented in this report, is a broadly applicable, proven model. It is intended for operational use and is applicable to any channel (branch) or system of channels (network of branches) subject to backwater flow, unsteady flow, or both, whether caused by the ocean tides, flood waves, seiches, wind, or man-induced regulation. It may be implemented after data for the appropriate channel geometry and initial conditions descriptive of a prototype are obtained and when sequences of synchronous, precisely timed, boundary-value data are provided at its boundary extremities. The model is designed to efficiently compute unsteady flow and water-surface elevation of either singular or interconnected channels. In general, a prototype waterway may be as simple as one channel with an appropriate set of boundary-value data defined at its extremities or as complex as a system of interconnected channels offering multiple flow paths and requiring boundary-condition definition at several external locations. A typical network composed of branches (reaches) and segments (subreaches) is illustrated in figure 1. Although the flow rates and water-surface elevations that occur at the end points of each of the segments could be computed directly, an important feature of this model is the incorporation of a transformation technique that results in a very significant savings in required computer time and storage. The transformation is accomplished by grouping the segments into branches, forming a transformation equation to relate the unknowns between consecutive segments within a branch, and using the resultant branch-transformation equations to form a coefficient matrix much reduced in size over what would otherwise be the case. Model flexibility permits the user to define segments and branches as may be appropriate. Moreover, the user may designate tributary inflows at internal junctions since boundary compatibility conditions at all such junctions are resolved automatically.

Aspects of the model and its implementation are presented in a thorough yet concise manner. In this regard it is assumed that the model user has an elementary knowledge of the hydromechanics of open-channel flow, of finite-difference methods for solving partial-differential equations, and of matrix algebra. Moreover, a basic familiarity with

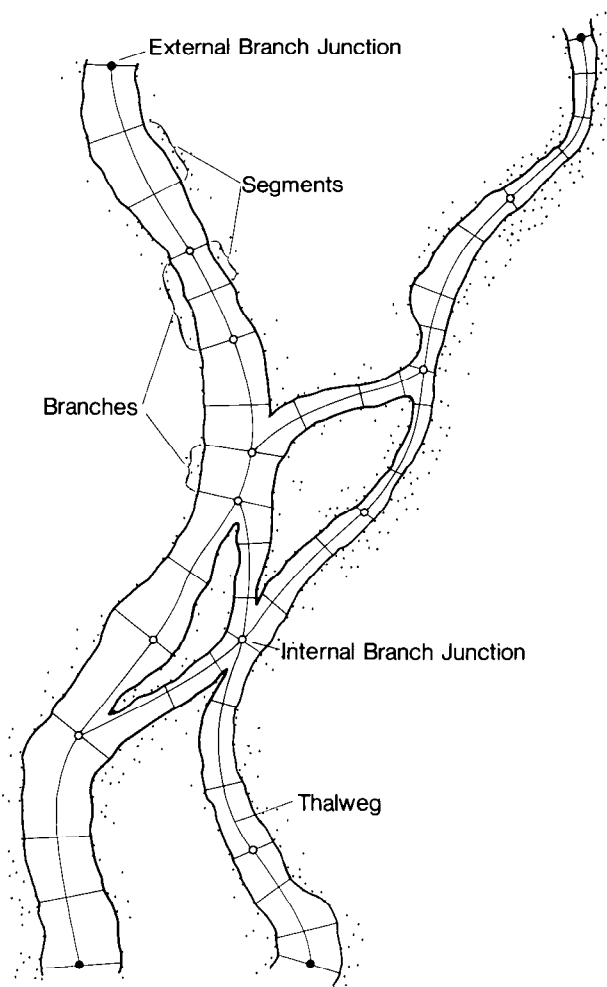


FIGURE 1.— Definition schematic of a hypothetical network.

modern computers and their operating systems and with the FORTRAN IV programming language is presumed.

The discussions of channel properties, cross-sectional geometry, initial and boundary-value data, computational control parameters, and model calibration and verification are intended to be reasonably self-contained. The effects of selecting different computational weighting factors and of inadvertently using various types of errant data are illustrated for a calibrated model of one particular prototype flow system. The structure, manner of operation, and input of data to the branch-network-model program—replete with operational examples—are fully documented. A listing of the current version of the computer program is presented in Appendix IV of this report. Inherent program limitations, resulting primarily as a con-

sequence of a priori selection of array dimensions do exist, necessarily, and are identified. However, the program may be easily modified to accommodate prototype networks having unique dimension requirements. The model user is specifically informed what variables must be adjusted to effect such changes.

The ultimate usefulness of a simulation model depends in large measure on two factors: first, its adaptability to a broad variety of prototype conditions and, second, the ease with which it can be implemented, modified to reflect changes to the prototype, and used to generate results that can be comprehended easily and quickly. Tabular listings and digital-graphic plots, illustrating some of the available output formats, are presented for five different applications of the model depicting a broad scope of prototype conditions.

Acknowledgments

The authors hereby express their appreciation for the assistance of their colleagues at U.S. Geological Survey field offices in California, Connecticut, Idaho, Michigan, and Washington, who were responsible in large measure for the collection of the prototype data used in this report. The authors are grateful, also, to the many Federal, State, and local governmental agencies in each of those States who, through their cooperation with the U.S. Geological Survey, have contributed financially to the collection of these data.

The water-level data used in the development of the flow model of the Detroit River were provided by the National Ocean Survey, National Oceanic and Atmospheric Administration. The cooperation of our colleagues in the National Ocean Survey in making these data available to us is gratefully appreciated.

Unsteady-Flow Equations for Networks of Open Channels

Flow equations

The one-dimensional partial-differential equations governing transient flow in open channels

have been reported previously in the literature (Baltzer and Lai, 1968; Dronkers, 1964, 1969; Strelkoff, 1969; Yen, 1973). The system of differential equations presented by Baltzer and Lai constitutes the basis for the open-channel-network flow equations. Using the water-surface elevation, Z , and the channel discharge, Q , as dependent variables, the equation of continuity can be written as

$$B \frac{\partial Z}{\partial t} + \frac{\partial Q}{\partial x} = 0,$$

in which B is the channel top width, as shown in figure 2. The distance, x , in the longitudinal direction and the elapsed time, t , are the independent variables. The equation of motion for one-dimensional open-channel flow can be obtained as

$$\frac{\partial Q}{\partial t} + \frac{Q}{A} \frac{\partial Q}{\partial x} + Q \frac{\partial(Q/A)}{\partial x} + gA \frac{\partial Z}{\partial x} + \frac{gk}{AR^{4/3}} Q|Q| = 0,$$

in which g is the acceleration of gravity, A is the cross-sectional area, R is the hydraulic radius, and k is a function of the flow-resistance coefficient, η (similar to Manning's n), which can be expressed in the inch-pound system of units as

$$k = \left(\frac{\eta}{1.49} \right)^2 \quad (\text{or in the metric system as } k = \eta^2).$$

When wind effect is taken into consideration the equation of motion becomes

$$\frac{\partial Q}{\partial t} + \frac{Q}{A} \frac{\partial Q}{\partial x} + Q \frac{\partial(Q/A)}{\partial x} + gA \frac{\partial Z}{\partial x} + \frac{gk}{AR^{4/3}} Q|Q| - \xi BU_a^2 \cos \alpha = 0,$$

in which U_a is the wind velocity vector making an angle α with the positive x -axis and ξ is a dimensionless wind-resistance coefficient, which can be expressed as a function of the water-surface drag coefficient, C_d , the water density, ρ , and the air density, ρ_a , as

$$\xi = C_d \frac{\rho_a}{\rho}.$$

The applicability of these equations is governed by several underlying assumptions that arise in the derivation process. Specifically, the slope of the channel bottom must be mild and

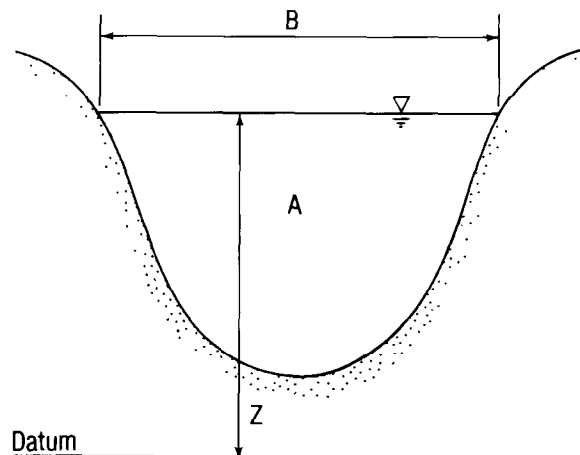


FIGURE 2. — Definition sketch of a channel cross section.

reasonably constant over the reach length, so that the flow remains subcritical. Lateral flow into or out of the channel must be negligible between channel junctions. The Manning formula is assumed to provide an accurate approximation of the frictional-resistance force for unsteady as well as steady flow. Furthermore, it is assumed that flow in the channel is substantially homogenous in density, that hydrostatic pressure exists everywhere in the channel, and that a uniform velocity distribution prevails throughout any cross section.

Since the flow velocity in most natural rivers and waterbodies typically varies throughout the cross section, a more realistic set of flow equations can be obtained by re-examining the equation of motion, thereby seeking to relax the uniform-velocity-distribution assumption. From a statistical analysis of turbulent flow behavior, one finds that the instantaneous flow velocity at a point consists of the mean velocity for the cross section plus the local component of deviation from the mean. When the velocity distribution over the channel cross section becomes highly nonuniform, it becomes necessary to account for these velocity deviations in the equation of motion. Taking into account these velocity fluctuations, one derives the following form of the equation of motion (Schaffranek, 1976):

$$\frac{\partial Q}{\partial t} + \beta \frac{Q}{A} \frac{\partial Q}{\partial x} + Q \frac{\partial(\beta Q/A)}{\partial x} + gA \frac{\partial Z}{\partial x} + \frac{gk}{AR^{4/3}} Q|Q| - \xi BU_a^2 \cos \alpha = 0,$$

where β , known as the momentum or Boussinesq coefficient, can be expressed as

$$\beta = \frac{\int u^2 dA}{U^2 A}.$$

In this relationship, derived from the conservation of momentum principle, u represents the velocity of water passing through some finite elemental area, dA , U is the mean velocity in the cross section, and A is the cross-sectional area as previously defined. In the equation the variation of β with respect to longitudinal distance is assumed to be negligible.

For channels of regular cross section and fairly straight channel alinement, it may be reasonable to neglect the minor effect of the nonuniform velocity distribution by setting the momentum coefficient equal to one. That this is possible for such channels is due primarily to the diminished significance of this effect as opposed to the effects of inaccuracies in determining the channel schematization, as well as the bottom and surface friction coefficients. In reality, however, the momentum coefficient for flows in natural rivers and waterbodies will always be greater than unity. It is generally found that the value of β for fairly straight prismatic channels ranges approximately from 1.01 to 1.12 (see Chow, 1959). Generally, the coefficient is larger for small channels and smaller for large channels of considerable depth. Consequently, the above equation of motion for a nonuniform velocity distribution is utilized to broaden the scope of applicability of the flow model.

Further reduction of the equation of motion results in a form more amenable to finite-difference approximation. Factoring the equation and separating the derivative of the quotient in the third term, one can obtain the following form:

$$\frac{1}{gA} \frac{\partial Q}{\partial t} + \frac{2\beta Q}{gA^2} \frac{\partial Q}{\partial x} - \frac{\beta Q^2}{gA^3} \frac{\partial A}{\partial x} + \frac{\partial Z}{\partial x} + \frac{k}{A^2 R^{4/3}} Q|Q| - \frac{\xi B}{gA} U_a^2 \cos \alpha = 0.$$

This equation and the equation of continuity, restated for convenience,

$$B \frac{\partial Z}{\partial t} + \frac{\partial Q}{\partial x} = 0,$$

represent the flow equations utilized in the branch-network flow model.

Boundary conditions

Solution of the flow equations requires specification of boundary conditions throughout the duration of the simulation at the physical extremities of the network, as well as at branch junctions within the network. Equations describing the boundary conditions at branch junctions are automatically generated by the branch-network-model program, whereas boundary-condition equations for the network extremities are derived from user-supplied time histories of boundary-value data or formulated from user-specified functions.

Compatibility conditions at internal junctions

The most common boundary condition encountered in networks of interconnected channels occurs at junctions where two or more branches join. This situation typically occurs where a channel is joined by a tributary or where a channel is divided by the presence of an island. At such internal junctions, stage (water-surface elevation) and discharge compatibility conditions must be satisfied. By neglecting velocity differences and energy losses due to turbulence at the junctions, appropriate compatibility conditions can be specified. For a junction composed of n branches, discharge continuity requires that

$$\sum_{m=1}^n Q_m = W_k,$$

where W_k is some specified external flow at junction k . Since the stage at a junction is single valued, stage compatibility equations are applied as follows:

$$Z_m = Z_{m+1}, m = 1, 2, \dots, (n-1).$$

Therefore, at an internal junction of n branches there are one discharge continuity and $n-1$ stage compatibility conditions that must be satisfied.

Boundary conditions at external junctions

In addition to the required boundary conditions at internal junctions, boundary conditions must be specified at all external junctions, that is, junctions with a singular connecting branch as identified in figure 1. Various combinations of boundary conditions can be specified at the

external junctions of a network. External boundary conditions can consist of a zero discharge (as, for example, at a dead-end branch), known discharge as a function of time, known stage as a function of time, or a known unique stage-discharge relationship. Boundary conditions, defined by time-sequences of discrete boundary-value data, can be made available to the branch-network flow model via punched computer cards or from computer data files of the direct-access type.

Initial conditions

In order to initiate a solution of the system of equations with the specified boundary conditions, initial values of the unknown quantities are required. These values may be obtained from measurements, computed from some other source, such as steady-state approximations, or computed from previous simulations. Successive use of the newly computed values as initial values permits the computation to proceed step-by-step until the boundary-value data are exhausted or the simulation is otherwise terminated. Successful convergence of the computation to the correct solution requires that the initial values be reasonably accurate; the less accurate the initial values, the longer the computation takes to dissipate the initialization error and converge to the true solution.

Solution Technique for Open-Channel Network Flow Simulation

The set of nonlinear partial-differential equations describing unsteady flow in open-channel networks defies analytical solution. Approximate solutions can be obtained by replacing the partial-differential equations by appropriate finite-difference expressions. In the branch-network flow model a weighted, four-point, finite-difference scheme is employed, and the resultant system of algebraic equations is solved simultaneously. This weighted, four-point, implicit-solution technique is used because of its

inherent computational efficiency, stability, and versatility with respect to the application of boundary conditions.

Finite-difference formulation

Formulation of the finite-difference equations consists of treating time derivatives of the dependent variables, stage and discharge, as centered both in space and in time and of treating spatial derivatives of the dependent variables as centered in space and positioned in time according to a user-defined weighting factor. The lone exception is the spatial derivative of the cross-sectional area in the equation of motion, which is approximated by a forward-difference technique. The geometric properties of area, top width, and hydraulic radius, as well as the discharges in nonderivative form in the equation of motion, are treated as weighted, four-point, difference quantities in a fashion similar to the approximation of the spatial derivatives of the dependent variables. (Discrete values of the hydraulic radius are approximated by the hydraulic depth, which is the cross-sectional area divided by the channel top width.) Thus, these functional values can be approximated at the time level at which the spatial derivatives are defined or at any other different level within the time interval.

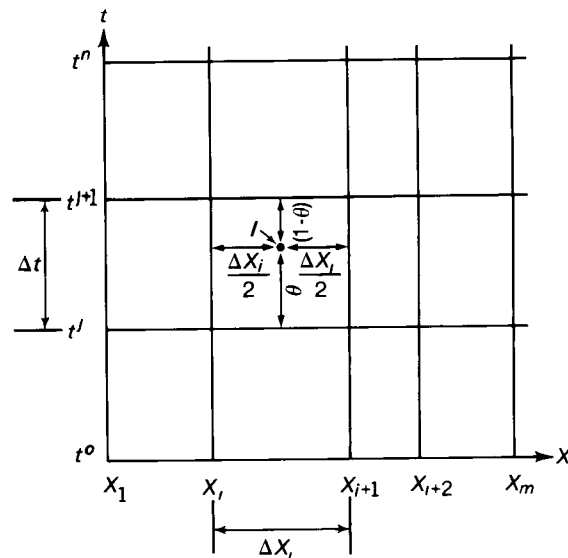


FIGURE 3. — Space-time-grid system for finite-difference approximations.

As can be seen from the space-time-grid system shown in figure 3, the four points used in the approximations are identified by the intersections of the vertical lines at distances x_i and x_{i+1} with the horizontal lines representing the time levels at t^j and t^{j+1} . The computational scheme uses a fixed time step, Δt , but permits the subdivision of branches into segments of equal or unequal lengths. In the finite-difference approximations, Δx_i represents the length of the i th segment of any given branch. From the space-time-grid system of figure 3, time and space derivatives of the functional value, $f(I)$, are approximated, respectively, as follows:

$$\frac{\partial f(I)}{\partial t} \approx \frac{f_{i+1}^{j+1} + f_i^{j+1} - f_{i+1}^j - f_i^j}{2\Delta t},$$

and

$$\frac{\partial f(I)}{\partial x} \approx \theta \frac{f_{i+1}^{j+1} - f_i^{j+1}}{\Delta x_i} + (1-\theta) \frac{f_{i+1}^j - f_i^j}{\Delta x_i}.$$

In the approximation of the spatial derivatives, $f(I)$ represents the dependent variables, stage and discharge, and θ is a weighting factor determining the time between the t^j and t^{j+1} time lines at which the spatial derivatives are evaluated. The spatial derivative of the cross-sectional area in the equation of motion is approximated by a forward-difference technique as

$$\frac{\partial A}{\partial x} \approx \frac{A_{i+1}^{j+1} - A_i^{j+1}}{\Delta x_i}.$$

In a manner similar to the treatment of the spatial derivatives, quantities such as the cross-sectional area, top width, hydraulic radius, and the discharge in nonderivative form in the equation of motion, represented by $f(I)$, are approximated by

$$f(I) \approx \chi \frac{f_{i+1}^{j+1} + f_i^{j+1}}{2} + (1-\chi) \frac{f_{i+1}^j + f_i^j}{2}.$$

In this expression χ is a weighting factor, similar to θ , specifying the time at which these functional quantities are evaluated between the t^j and t^{j+1} adjacent time levels at the midpoint of the i th segment.

In the four-point, finite-difference scheme, θ is a real constant, generally thought of as lying in the interval $0 \leq \theta \leq 1$. If θ is not zero, one must solve a set of simultaneous linear equations, and therefore it is called an implicit system. When θ

is less than 0.5 the four-point, implicit, finite-difference equations are found to be conditionally linearly stable. The equations are found to be unconditionally linearly stable when θ is greater than or equal to 0.5 and less than or equal to 1.0. A weighting factor value of 0.5 yields the traditional box scheme used by Preissman (1960) and by Amein and Fang (1970), whereas a θ value of 1.0 represents the fully forward scheme presented by Baltzer and Lai (1968).

The weighting factor χ is similarly taken as lying in the interval $0 \leq \chi \leq 1$. If χ is zero, function values are determined exclusively from previous time step quantities, whereas a χ weighting factor of one produces a fully forward approximation of the applicable functions.

Computational effects of various values for the θ and χ weighting factors are discussed in subsequent sections, and appropriate value ranges are suggested. Stability and other numerical properties of the four-point, implicit, finite-difference scheme are also discussed in detail by Fread (1974).

Utilizing these finite-difference approximations and the notation $\tilde{f}(I)$ to signify function values derived from the previous iteration, one can transform the partial-differential flow equations into the following finite-difference expressions for the i th segment: for the continuity equation,

$$\tilde{B} \left[\frac{Z_{i+1}^{j+1} + Z_i^{j+1}}{2\Delta t} - \frac{Z_{i+1}^j + Z_i^j}{2\Delta t} \right] + \theta \frac{Q_{i+1}^{j+1} - Q_i^{j+1}}{\Delta x_i} + (1-\theta) \frac{Q_{i+1}^j - Q_i^j}{\Delta x_i} = 0,$$

and for the equation of motion,

$$\begin{aligned} & \frac{1}{g\tilde{A}} \left[\frac{Q_{i+1}^{j+1} + Q_i^{j+1}}{2\Delta t} - \frac{Q_{i+1}^j + Q_i^j}{2\Delta t} \right] \\ & + \frac{2\beta\tilde{Q}}{g\tilde{A}^2} \left[\theta \frac{Q_{i+1}^{j+1} - Q_i^{j+1}}{\Delta x_i} + (1-\theta) \frac{Q_{i+1}^j - Q_i^j}{\Delta x_i} \right] \\ & - \frac{\beta\tilde{Q}^2}{g\tilde{A}^3} \frac{\tilde{A}_{i+1}^{j+1} - \tilde{A}_i^{j+1}}{\Delta x_i} + \theta \frac{Z_{i+1}^{j+1} - Z_i^{j+1}}{\Delta x_i} + (1-\theta) \frac{Z_{i+1}^j - Z_i^j}{\Delta x_i} \\ & + \frac{k|\tilde{Q}|}{\tilde{A}^2\tilde{R}^{4/3}} \left[\chi \frac{Q_{i+1}^{j+1} + Q_i^{j+1}}{2} + (1-\chi) \frac{Q_{i+1}^j + Q_i^j}{2} \right] \\ & - \frac{\xi\tilde{B}}{g\tilde{A}} U_a^2 \cos \alpha = 0. \end{aligned}$$

In this solution technique stage and discharge are computed at the ends of the segments identified by the i and $i+1$ locations. The equations consist of four unknown quantities represented by Z_{i+1}^{j+1} , Z_i^{j+1} , Q_{i+1}^{j+1} , and Q_i^{j+1} . Therefore, as it exists, the equation set is indeterminate since the two equations have four unknowns. However, with suitable boundary conditions specified, the number of equations can be increased in order that a solution can be effected by implicit means.

Coefficient-matrix formulation

Solution of the flow equations is conveniently accomplished by matrix methods after appropriate coefficient matrices are constructed. Rewriting the continuity equation as

$$Q_{i+1}^{j+1} - Q_i^{j+1} + \frac{(1-\theta)}{\theta} (Q_{i+1}^j - Q_i^j) + \frac{\tilde{B}\Delta x_i}{2\Delta t\theta} (Z_{i+1}^{j+1} + Z_i^{j+1} - Z_{i+1}^j - Z_i^j) = 0,$$

and letting

$$\gamma = \frac{\tilde{B}\Delta x_i}{2\Delta t\theta},$$

one derives the desired coefficient form of the continuity equation in terms of the four unknowns for the i th segment,

$$Q_{i+1}^{j+1} + \gamma Z_{i+1}^{j+1} - Q_i^{j+1} + \gamma Z_i^{j+1} = \delta,$$

wherein

$$\delta = -\frac{(1-\theta)}{\theta} (Q_{i+1}^j - Q_i^j) + \gamma (Z_{i+1}^j + Z_i^j).$$

In a like manner, the coefficient form of the equation of motion can be derived from the previously formulated finite-difference equation. After it is factored, the equation of motion for the i th segment can be written,

$$\begin{aligned} & \frac{\Delta x_i}{2\Delta t\theta g\tilde{A}} [Q_{i+1}^{j+1} + Q_i^{j+1} - Q_{i+1}^j - Q_i^j] \\ & + \frac{2\beta\tilde{Q}}{g\tilde{A}^2} \left[Q_{i+1}^{j+1} - Q_i^{j+1} + \frac{(1-\theta)}{\theta} (Q_{i+1}^j - Q_i^j) \right] \\ & + Z_{i+1}^{j+1} - Z_i^{j+1} + \frac{(1-\theta)}{\theta} (Z_{i+1}^j - Z_i^j) \\ & + \frac{\chi\Delta x_i k|\tilde{Q}|}{2\theta\tilde{A}^2\tilde{R}^{4/3}} \left[Q_{i+1}^{j+1} + Q_i^{j+1} + \frac{(1-\chi)}{\chi} (Q_{i+1}^j + Q_i^j) \right] \end{aligned}$$

$$= \frac{\beta\tilde{Q}^2}{\theta g\tilde{A}^3} (\tilde{A}_{i+1}^{j+1} - \tilde{A}_i^{j+1}) + \frac{\xi\Delta x_i\tilde{B}}{\theta g\tilde{A}} U_a^2 \cos \alpha.$$

With the definition of the coefficients,

$$\lambda = \frac{\Delta x_i}{2\Delta t\theta g\tilde{A}}, \quad \mu = \frac{2\beta\tilde{Q}}{g\tilde{A}^2}, \quad \text{and} \quad \sigma = \frac{\chi\Delta x_i k|\tilde{Q}|}{2\theta\tilde{A}^2\tilde{R}^{4/3}},$$

the equation of motion, after substitution and collection of terms, becomes

$$(\lambda + \sigma) [Q_{i+1}^{j+1} + Q_i^{j+1}] + \mu [Q_{i+1}^{j+1} - Q_i^{j+1}] + [Z_{i+1}^{j+1} - Z_i^{j+1}] = \epsilon,$$

wherein

$$\begin{aligned} \epsilon = & \left(\lambda - \sigma \frac{(1-\chi)}{\chi} \right) [Q_{i+1}^j + Q_i^j] \\ & - \mu \frac{(1-\theta)}{\theta} [Q_{i+1}^j - Q_i^j] - \frac{(1-\theta)}{\theta} [Z_{i+1}^j - Z_i^j] \\ & + \frac{\beta\tilde{Q}^2}{\theta g\tilde{A}^3} [\tilde{A}_{i+1}^{j+1} - \tilde{A}_i^{j+1}] + \frac{\xi\Delta x_i\tilde{B}}{\theta g\tilde{A}} U_a^2 \cos \alpha. \end{aligned}$$

Finally, with the substitutions $\zeta = \lambda + \sigma + \mu$ and $\omega = \lambda + \sigma - \mu$, the coefficient form of the equation of motion in the four unknown quantities for the i th segment can be written as

$$\zeta Q_{i+1}^{j+1} + Z_{i+1}^{j+1} + \omega Q_i^{j+1} - Z_i^{j+1} = \epsilon.$$

Together with the continuity equation derived previously as

$$Q_{i+1}^{j+1} + \gamma Z_{i+1}^{j+1} - Q_i^{j+1} + \gamma Z_i^{j+1} = \delta,$$

the flow equations for the i th segment can be expressed in the following matrix form

$$\begin{bmatrix} 1 & \zeta \\ \gamma & 1 \end{bmatrix} \begin{bmatrix} Z_{i+1}^{j+1} \\ Q_{i+1}^{j+1} \end{bmatrix} - \begin{bmatrix} 1 & -\omega \\ -\gamma & 1 \end{bmatrix} \begin{bmatrix} Z_i^{j+1} \\ Q_i^{j+1} \end{bmatrix} = \begin{bmatrix} \epsilon \\ \delta \end{bmatrix}.$$

Branch-transformation equation

Using appropriate internal and external boundary conditions and initial values, one may effect a matrix solution directly for the set of flow equations for all segments within the network, a segment being the primary subdivision of a branch as shown in figure 1. The resultant solution set would consist of computed values of stage and discharge at all cross sections delineating the segments. However, the equation set of a network consisting of M segments would form a coefficient matrix of minimum order

$2M + 2$ requiring solution at each time step. For instance, a network composed of 10 sequentially connected branches, each subdivided into 5 segments (50 segments in all) would require a 102×102 size coefficient matrix of 10,404 computer-word locations to hold the equation set. Since the computer costs necessary to perform a solution for an equation set of this magnitude could be substantial, it is desirable to examine alternate means of formulating the coefficient matrix.

From the coefficient matrices of the finite-difference equations a transformation equation can be obtained that defines the relationship between the unknowns at consecutive cross sections that delimit a branch segment. By coupling all segment-transformation equations for a branch, a transformation equation results that relates the unknowns at the termini of the branch. By using these branch-transformation equations instead of segment-flow equations, the size of the coefficient matrix is reduced to order $4N$ for a network of N branches. The above-mentioned, ten-branch system, having five segments per branch, would then require only a 40×40 size coefficient matrix of 1,600 computer-word locations. Obviously, the result is a significant savings in computer costs because of reduced computational time and computer storage demands. Values of water-level and discharge at the cross sections delineating the segments within each branch are subsequently derived by back substitution.

Defining a two-component vector of state at the i th cross section,

$$S_i^{j+1} = \begin{bmatrix} Z_i^{j+1} \\ Q_i^{j+1} \end{bmatrix},$$

one may write the following transformation equation for the i th segment from the vector of state for the cross section at the $i + 1$ location,

$$S_{i+1}^{j+1} = U_{(i)} S_i^{j+1} + u_{(i)}.$$

The transformation matrices of the i th segment, $U_{(i)}$ and $u_{(i)}$, follow from the previously defined coefficient matrices thusly:

$$U_{(i)} = \begin{bmatrix} 1 & \zeta_{(i)} \\ \gamma_{(i)} & 1 \end{bmatrix}^{-1} \begin{bmatrix} 1 & -\omega_{(i)} \\ -\gamma_{(i)} & 1 \end{bmatrix}$$

and

$$u_{(i)} = \begin{bmatrix} 1 & \zeta_{(i)} \\ \gamma_{(i)} & 1 \end{bmatrix}^{-1} \begin{bmatrix} \epsilon_{(i)} \\ \delta_{(i)} \end{bmatrix}.$$

A branch-transformation equation can now be obtained through successive application of the segment-transformation equation. The resulting equation relates the unknowns at cross sections 1 and m of the n th branch,

$$S_m^{j+1} = U_n S_1^{j+1} + u_n,$$

wherein the transformation matrices of the n th branch, U_n and u_n , are obtained through successive substitution of the segment-transformation equation from the $m - 1$ segment down to the first segment. These branch-transformation matrices,

$$U_n = U_{(m-1)} U_{(m-2)} \cdots U_{(1)}$$

and

$$u_n = u_{(m-1)} + U_{(m-1)} (u_{(m-2)} + U_{(m-2)} (u_{(m-3)} \cdots + U_{(3)} (u_{(2)} + U_{(2)} u_{(1)}) \cdots)$$

describe the relationship between the vectors of state, S_1^{j+1} and S_m^{j+1} , at the ends of the branch, that is, at the junctions. After a matrix solution is effected producing the stages and discharges at junctions, intermediate values of the unknowns at additional cross sections that delimit the branch segments are successively computed using the segment-transformation equation for the particular branch.

Matrix solution

For a network of N branches, the branch-transformation equations, internal boundary conditions, and external boundary conditions form a linear system of $4N$ equations in $4N$ unknowns. Branch-transformation equations appear first in the matrix followed immediately by internal boundary equations and finally by the external boundary conditions expressed in equation form. The system of equations may be expressed in matrix notation as $AX = B$, where the coefficient matrix A is $4N \times 4N$, X is the vector of $4N$ unknowns, and B is the right-hand column vector of $4N$ constants.

For the hypothetical Y network illustrated in figure 4, the contents of the coefficient matrices

are shown in figure 5. The network consists of three branches (branches are identified by superscripts) joining at a single junction (junctions are indicated by subscripts). Boundary conditions at the three external junctions consist of known stage as a function of time. No external flow exists at the internal junction; stage and discharge compatibility conditions at this junction are as specified in the figure.

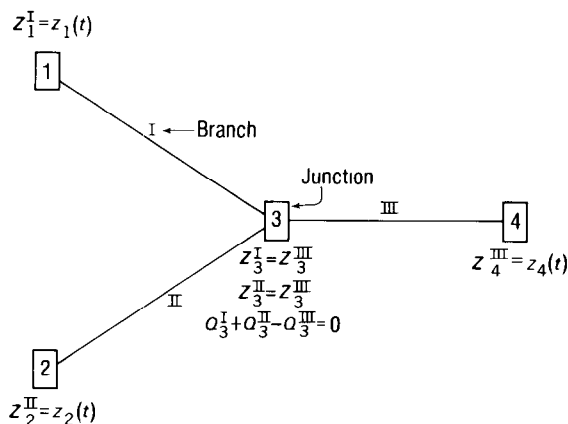


FIGURE 4.—A simple hypothetical network. (Superscripts identify branches; subscripts identify junctions.)

Numerous techniques exist for numerical solution of systems of linear equations such as illustrated in figure 5. One of the most widely used methods for solving simultaneous equations is Gaussian elimination. (The term "elimination" is derived from the process whereby unknowns are successively eliminated by combining equations.) Gaussian elimination is a two-step method. By successive combinations of equations, all of the coefficients in the *A* matrix below the diagonal are eliminated to form an upper triangular matrix. After the upper triangular matrix has been formed, the unknowns are determined by back substitution of lower equations into those higher in the matrix.

The equation used to eliminate the unknowns in the other equations is called the pivot equation. Roundoff errors in the elimination process can be minimized by choosing the equation having the largest coefficient in the column as the pivot equation. This technique, known as Gaussian elimination using maximum pivot strategy, is utilized to effect the matrix solution in the branch-network flow model.

$$A \times X = B$$

z_1^I	a_1^I	z_3^I	a_3^I	z_2^II	a_2^II	z_3^II	a_3^II	z_3^III	a_3^III	z_4^III	a_4^III
u_{11}^I	u_{12}^I	-1									
u_{21}^I	u_{22}^I		-1								
				u_{11}^II	u_{12}^II	-1					
				u_{21}^II	u_{22}^II		-1				
								u_{11}^III	u_{12}^III	-1	
								u_{21}^III	u_{22}^III		-1
		1									0
						1					0
			1				1				0
1											$z_1(t)$
				1							$z_2(t)$
										1	$z_4(t)$

FIGURE 5.—Coefficient matrices for the hypothetical network shown in figure 4.

Solution of the matrix results in determination of the stage and discharge at the termini of the branches (at the junction cross sections). Intermediate values of the unknowns at the termini of the segments (at cross sections located between junctions) are determined through successive application of the segment-transformation equation defined previously.

By use of the initial conditions, that is the values given at t^0 , to initiate the simulation, the computation proceeds step-by-step to the end of the simulation at t^n through successive solution of the coefficient matrices. The matrix coefficients contain known quantities at the present time level, t^j , as well as unknowns at the forward time level, t^{j+1} . Iterative solutions may be performed within the time step to refine the computed results and thereby satisfy the user-specified accuracy requirements. Present time-step quantities are obtained either as initial values (at the t^0 time level) or as the last solution values derived in the previous time step (at all subsequent time levels). Forward time-step quantities are obtained initially either from present values or by extrapolation and thereafter from the most recent values derived through iteration within the time step.

Branch-Network Model Implementation

In addition to the hydrodynamic factors governing the applicability of the one-dimensional flow equations, several fundamental considerations constrain flow analysis by one-dimensional methods of approximation. The most obvious constraint is that the individual channel geometry be sufficiently simple so as to lend itself to one-dimensional characterization. Specifically, the channels should be sufficiently "straight" in the longitudinal sense so that the flow may be simulated by flow in straight channels. Channels with bends of significant curvature may also be treated if determination of the flow field in the bend is not important. In this situation the influence of the curvature on the flow field may either be neglected, if deemed minor, or accounted for by means of appropriate values for the momentum and (or) flow-resistance coefficients. All artificial or natural section controls within the channels must be identified and taken into account in the model schematization.

Other constraints related to the water-surface profile are also significant in determining the suitability of a one-dimensional analysis. The water-surface profile at the boundary-value, data-collection locations must be horizontal in the transverse direction to insure proper determination of the water-surface elevations. Furthermore, the overall channel distance between external junctions must be sufficient to permit accurate determination of the longitudinal water-level variation so that adverse effects of measurement errors are minimized. This is particularly important if these measured data are to be used as boundary values or for calibration.

Certainly, many other factors may also enter into determination of the applicability of one-dimensional flow analyses. Some of these have been reported elsewhere by Schaffranek and Baltzer (1978). To attempt to list all the necessary considerations is not possible. However, certain implementation constraints of major concern will be identified as they arise subsequently.

Channel and Cross-Sectional Geometry

Implementation of the branch-network flow model necessitates determination of several physical and hydraulic properties of the prototype system under investigation. Certain of these properties are made readily available through direct field measurements. Others defy direct field quantification, thereby necessitating initial approximation and subsequent refinement throughout the model calibration and verification processes. Nevertheless, accurate flow computation requires proper definition of these properties in order to maintain compatibility with the one-dimensional analytical methods employed.

In order to implement the branch-network flow model it is necessary to accurately describe the prototype system under investigation. In this schematization process, it is essential to precisely identify the branch and junction locations, the branch and segment lengths, the cross-sectional geometry, and all other geometrical and physical properties that affect the flow. As a first step toward fulfilling these data requirements, a review of existing hydrologic and hydrographic information combined with a map and field reconnaissance of the prototype is an essential preliminary activity. This helps to define data collection requirements and field constraints and to determine the scope of the entire modeling effort.

Schematization of a network for flow simulation requires depicting the system by branches delimited by, and possibly connected at, junctions. Junctions are either internal or external to the network. (See fig. 1.) Locations at which two or more channels join or where nodal flow must be accommodated are internal junctions; model-defined boundary conditions supplemented by specified nodal flows are applied at these locations. Junctions at which a single branch is defined are external junctions; user-supplied boundary conditions are required at these locations. External junctions define the extremities of the network being simulated. In deciding upon the location of external junctions, it is, of course, economically advantageous to

establish their position so as to utilize data collected at existing field-station locations to satisfy boundary-condition requirements. However, where such data are not readily available and a location and means must be decided upon for acquiring the necessary boundary values, logistic and economic, as well as hydraulic considerations, play a significant role in the decision process. After junction locations are assigned, and the branches are thereby defined, a decision must be made whether or not to subdivide the branches into segments. Geometric and hydraulic factors, as well as computational considerations, are the basis upon which the subdivision of branches into segments is determined. Once the branches and segments have been delineated, their lengths can be determined by field surveys or by measuring along the channel thalweg as depicted on topographic maps or marine charts. (In one-dimensional analyses the x -axis is taken as either the thalweg or map centerline of the channel, and the y -axis is the cross-channel coordinate.)

Cross-sectional geometry must be defined at the termini of all segments. Cross-sectional information consists of stage-area and stage-width relationships supplied in tabular form. The required cross-sectional geometry can be approximated from hydrographic survey charts, such as may be available from the National Ocean Survey, NOAA, or from the U.S. Army, Corps of Engineers, or measured directly by standard hydrographic survey techniques. Direct field measurement is recommended to insure that the model accurately depicts the current prototype conditions.

Channel Conveyance Parameters

In addition to the channel and cross-sectional properties required to conduct flow simulations, definition of certain other channel parameters is critical. Accurate definition of the flow-resistance coefficient is always necessary. Proper specification of the velocity distribution (momentum) coefficient and the wind-shear, water-surface drag coefficient may also be required depending on the particular flow conditions. While it is often difficult to quantify these

parameters precisely, reasonable approximations are obtainable.

Of the channel parameters identified, perhaps the most difficult to quantify is the flow-resistance coefficient. This is particularly true since the flow-resistance coefficient is typically a compound function of the physical and hydraulic properties of the channel. Thus, the flow-resistance coefficient, although principally dependent on the channel roughness, may be affected by inherent minor inaccuracies in the chosen schematization of the prototype. Complex networks also compound the problems associated with determination of the flow-resistance coefficient.

As stated in the section Flow equations, the Manning equation for steady uniform flow is assumed to provide a reasonable approximation of the frictional resistance expected for unsteady flow. In the Manning equation,

$$U = \frac{1.49}{\eta} R^{2/3} S^{1/2}$$

or, in the metric system,

$$U = \frac{1}{\eta} R^{2/3} S^{1/2}$$

R is the hydraulic radius, S is the slope of the energy gradient, U is the velocity and η is the flow-resistance coefficient. The flow-resistance coefficient notation, η , is used in place of Manning's n to indicate, first, that the coefficient represents an unsteady flow situation and, second, that it may also be accounting for schematization inaccuracies. However, the flow-resistance coefficient should never exceed reasonable bounds. In fact, it should never vary greatly from its corresponding steady-flow approximation determined from the Manning equation. Such deviation, should it occur, must be interpreted as a signal of trouble and is very probably indicative of inappropriate use of one-dimensional techniques, schematization and (or) data inaccuracies, or excessive distortion of the prototype in the chosen schematization.

Accurate determination of the flow-resistance coefficient is often difficult. For unsteady-flow computation in a channel or network in which approximately steady-flow conditions occur, an η value equivalent to Manning's n , determined by the foregoing equation, may be used. For the

more difficult situation where steady-flow or nearly steady-flow conditions never prevail, the flow-resistance coefficient may be obtainable only by a trial-and-error process beginning with an initial estimate and successively adjusting the value until satisfactory flow results are achieved. If measured discharges are available, it is also possible to numerically compute η by methods described by Baltzer and Lai (1968).

Often flow resistance varies under changing flow conditions. It may be necessary, therefore, to treat the flow-resistance coefficient as a function of time. For example, it has been shown that the flow-resistance coefficient frequently varies with the Reynolds number (Baltzer and Lai, 1968). The variable behavior of the flow-resistance coefficient has also been linked to changes in the bed regime of the channel bottom or to extreme changes in the water temperature. Similar correlations of the flow-resistance coefficient have been detected and reported by others. Therefore, in the branch-network flow model the flow-resistance coefficient can be defined as a linear or quadratic function of the water temperature, discharge, flow depth, Froude number, or Reynolds number.

Accurate simulation of the flow conditions may also necessitate evaluation of the momentum coefficient as defined in the section Flow equations. This may be required for channels characterized by contractions and (or) expansions, meandering paths of travel, or cross-sectional irregularities, such as islands, sand bars, or gullies. In such highly nonprismatic or curved channels a uniform velocity distribution does not exist.

Evaluation of the momentum coefficient may be accomplished directly from field-measured horizontal and vertical velocity profiles by use of the integral definition. However, if available data are insufficient to determine the coefficient directly, other velocity distribution profiles may be examined and used to approximate the coefficient and thereby produce more accurate flow results than would otherwise be possible under the uniform-velocity-distribution assumption. In order to effect an approximation it is important to note that the momentum coefficient for the cross-sectional area is separable into two components accounting for the transverse and ver-

tical deviations of the velocity from their respective mean values. The momentum coefficient for the cross-sectional area is the product of these individual components (Schaffranek, 1976). Various semiempirically based theories have been proposed that provide accurate, realistic, laboratory- and field-substantiated approximations to the vertical velocity profile of natural channels and waterways; examples include Prandtl's mixing length theory, G. I. Taylor's vorticity transfer theory, and Von Kármán's similarity hypothesis. Similarly, more accurate approximation methods, such as exponential or logarithmic distribution forms, are available to depict the transverse distribution of flow in natural channels. Accurate evaluation of the momentum coefficient by realistic definition of the transverse and vertical flow distribution will obviously serve to improve the accuracy of the flow computations. The momentum coefficient is always greater than or equal to one; a value of one implies a uniform velocity distribution. For the turbulent flows typical of most natural channels, the momentum coefficient is on the order of 1.06.

Under some conditions it may also be necessary to account for wind-induced currents caused by wind stress acting on the water surface within the network. Thus, wind has been included as a forcing function in the branch-network flow equations. Evaluation of the wind effect requires specification of the air and water densities, the wind speed and direction (usually measured at standard anemometer height), and a water-surface drag coefficient. The difficulty in accurately simulating wind effect rests with selection of the most suitable value for the water-surface drag coefficient. Experimentation has shown that the value of this coefficient depends not only on the flow depth but also on the height, steepness, and celerity of the wind-generated surface waves. Representative values of the water-surface drag coefficient appear to range between 1.5×10^{-3} for light winds and 2.6×10^{-3} for strong winds (Wilson, 1960). Determination of the appropriate value may require analysis of the flow under various wind conditions. Plots of the water-surface drag coefficient versus wind speed are illustrated in Neumann and Pierson (1966).

Initial and boundary-value data

Three comprehensive sets of data are required to carry out flow simulations by mathematical-numerical models such as the branch-network flow model. Initial-condition data, channel geometry, and boundary-value data (usually water-surface elevations precisely timed and synchronized) constitute mandatory data requirements for flow computation by the branch-network flow model.

In addition to the required channel and cross-sectional data, which were described in the section Channel and cross-sectional geometry, initial values of the unknown quantities must be determined and supplied as initial conditions. As mentioned in the section Initial conditions, these values consisting of water-surface elevations and discharges at the termini of all segments can be obtained directly by field measurement, computed from previous simulations, approximated from some other source (such as assumed steady-state conditions), or simply estimated. By use of unsteady-flow data for the Sacramento River, model convergence for various deviations of the initial discharge from its true value is illustrated in figure 6. For initial values that are in error by as much as 100 percent the convergence time of the model is found to be roughly 2 hours (eight time steps) with a maximum deviation of 12.5 percent after five time steps (1 $\frac{1}{4}$ hours). At 0200 hours, 2 hours after the start of the simulation, all computed discharges are within 2 percent of the true value. Thus, while reasonable initial conditions are desirable, estimates can be used for starting conditions if a sufficient amount of "warmup" time is provided for the model to dissipate the errors and converge to the true solution. It is noteworthy that models of flow systems having high rates of energy dissipation will converge more rapidly than those having low rates of energy dissipation (Lai, 1965a, b).

Boundary conditions for the branch-network flow model consist of two types. First, stage and discharge compatibility conditions must be satisfied at junctions where two or more branches join internal to the network. Assignment of internal boundary conditions is accomplished automatically by the branch-network-model program. Using branch and

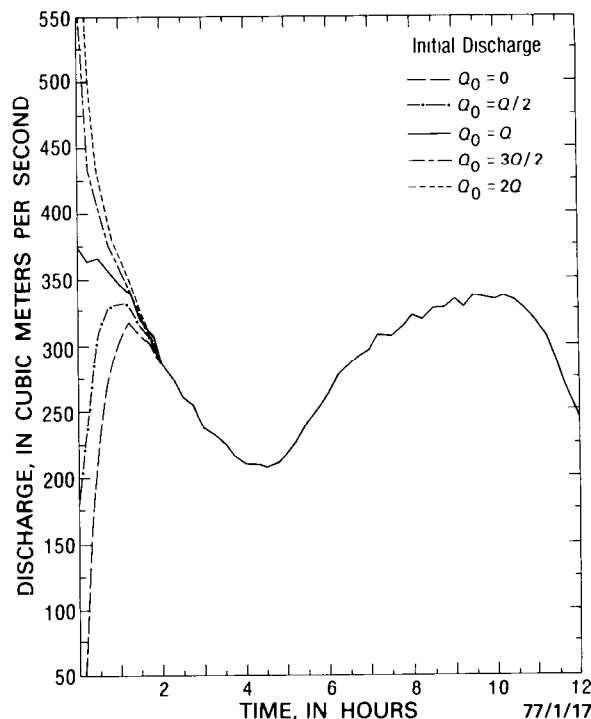


FIGURE 6.—Discharges computed for the Sacramento River near Freeport, Calif., by use of various initial values in the branch-network flow model.

junction identification information provided as input parameters, the program constructs the internal boundary-condition equations and fills the appropriate elements of the coefficient matrices with values describing these boundary conditions.

The second type of boundary condition must be defined by the model user. Such boundary conditions occur at the external junctions of the network, that is, at a junction consisting of a singular connecting branch. External boundary values may be specified either as a stage hydrograph or a discharge hydrograph or be prescribed by a unique stage-discharge relationship. The most commonly used external boundary condition is the stage hydrograph, since precise synchronous recording of the water-surface elevations can be accomplished automatically. Digital recorders actuated by a float or by a gas back-pressure servomanometer and timed by precision crystal timers encode these data on 16-channel punched-paper tapes at preselected time intervals. Subsequently, these punched-paper tapes of field-recorded,

time-dependent data are read by optical means, and the data are telemetered for processing on the U.S. Geological Survey computer system. Transmitted data are concurrently translated to extended binary coded decimal (EBCDIC) characters and temporarily recorded on digital magnetic tape. The magnetic tape containing the transmitted time-dependent data, identified by field-station number, data recording frequency, and beginning and ending dates and times, is then ready for subsequent translation, editing, and filing. An array of computer programs, referred to as the time-dependent data processing system, is available for use to edit and file such time-dependent data in order to provide boundary conditions for one-, two-, and three-dimensional models of flow and (or) transport. After processing, these data are made readily available for direct inclusion in the branch-network flow model. They can be retrieved directly by the model from the edited time-dependent data base by identifying the field-station number, data type, recording frequency, dates, and times of interest on data-request program-control cards input to the model. For data recorded at frequencies different from the computational time increment used in the model, parabolic interpolation is performed by the model to determine values consistent with the chosen time step.

All significant external inflows and outflows of the network must also be determined and identified in the model implementation. Constant inflows and (or) outflows in the network are presently treated as occurring at branch junctions. Therefore, it may be necessary to "lump" lateral flow between junctions, such as bank seepage, and define it as a point source occurring at one or more appropriate junctions. In the model schematization, inflow is typically taken to be positive in sign.

Computation-control parameters

Flow simulation by the branch-network flow model requires specification of several parameters that principally control the numerical computation process. Determination of appropriate values for these computational-control parameters is important because they

have an effect on the accuracy, convergence, and stability of the model. Three primary considerations, critical with regard to controlling the numerical computation, are determination of the simulation time increment, definition of the segment lengths, and selection of appropriate finite-difference weighting factors. Other considerations, such as the accuracy of the initial conditions and the value of the tolerance limits, are also important aspects affecting the numerical computation process.

Numerical solution of the flow equations on a rectangular $x-t$ grid system, whether by explicit finite-difference techniques or by the method-of-characteristics technique, imposes a constraint on determination of the computational time increment based on definition of the segment lengths. This constraint is not applicable, however, in a rigorous mathematical sense, to the implicit solution technique, such as is employed in the branch-network flow model. Characteristic and explicit schemes are subject to the Courant restriction, which imposes the following constraint upon the time-increment to segment-length ratio

$$\frac{\Delta t}{\Delta x} \leq \frac{1}{|U \pm \sqrt{gH}|}$$

In this relationship Δt is the time increment, Δx is the distance increment (or segment length), U is the mean flow velocity, g is the acceleration of gravity, and H is the depth of flow. Adherence to this restriction is necessary in order to assure stable computational conditions when utilizing method-of-characteristics or explicit solution techniques. This restriction on the time increment can frequently cause characteristic and explicit solution schemes to require excessive amounts of computer time; for this reason implicit solution techniques offer distinct economical advantages. Nevertheless, the Courant condition, which is a function of the wave celerity ($c = \sqrt{gH}$) and the flow velocity, remains a valuable index when selecting a time increment for implicit solutions, as well. For a fixed length, the Courant condition restricts the time increment of characteristic and explicit solutions accordingly,

$$\Delta t \leq \frac{\Delta x}{|U \pm \sqrt{gH}|}$$

On the other hand, various numerical simulations using the branch-network flow model have remained stable for large time steps appreciably exceeding the value imposed by the Courant restriction. One must be aware, however, that increasing the time increment may also degrade the accuracy of the simulation and thereby render the results useless. The time step used in the branch-network flow model may safely exceed the Courant value by a factor of two to five without undue degradation of the computed results. However, each model implementation is unique; thus, the appropriate time increment should be judiciously determined. The amount by which the Courant condition can be safely exceeded is a function of the weighting factor, θ , and the ratio of the critical segment length to the primary, translatory wave length.

Several simulation results using various time steps are illustrated in figure 7. The flow shown in the illustration is for the Sacramento River near Freeport, Calif. This application of the branch-network flow model treats the Sacramento River between Sacramento and Freeport, Calif., as one branch. The total branch length is 17.4 km, and it is treated as a single segment in the model simulations. Stages recorded at Sacramento (station number 11-4475.00) and near Freeport (station number 11-4476.50) on January 17, 1977, and used as boundary-value data for the model, are shown in figure 8. For the given flow conditions—maximum flow velocity of 0.45 m/s and wave celerity of 7.0 m/s—the time increment imposed by the Courant condition is approximately 40 minutes. The model was run with time steps of 15 minutes, 1 hour, 2 hours, and 4 hours. The 15-minute time step abides by the Courant condition whereas the 1-hour, 2-hour, and 4-hour time steps are, respectively, 1.5, 3, and 6 times the Courant value. As can be seen from figure 7 the computation remains stable for all time steps tested. However, the simulation results obtained using the larger time steps may not be very usable and, in fact, present a rather crude approximation of the flow profile. Therefore, it is always important to select a time step that produces the best approximation of the flow conditions and, hence, the most usable results.

Oftentimes model output results are used for special purposes, such as to drive a transport

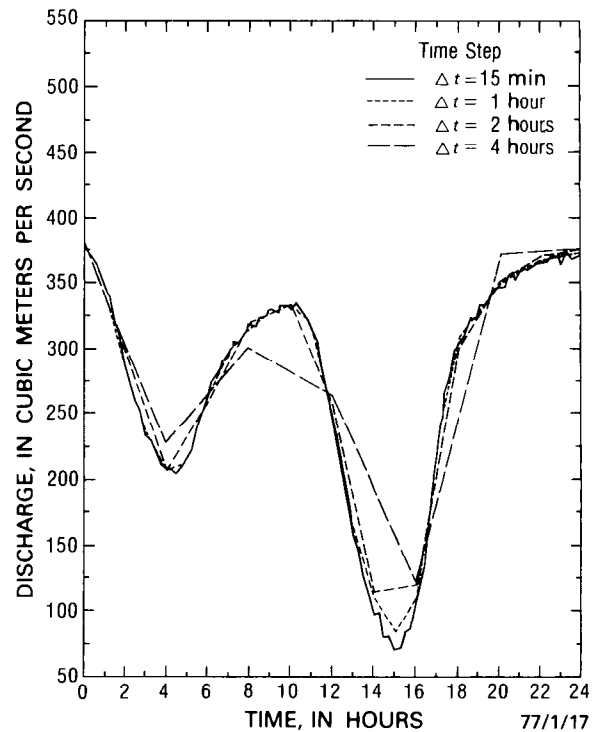


FIGURE 7.—Discharges computed for the Sacramento River near Freeport, Calif., by use of various time increments in the branch-network flow model.

model. This may require computation at some predetermined time increment. For this situation the segment lengths can also be selected using the Courant condition as an index. Usually in one-dimensional flow analyses the segment lengths are set on the order of 10 times the width. However, the segment length specification is primarily a function of the flow accuracy requirements.

Thus, although the time-step to segment-length ratio presented by the Courant condition need not be strictly upheld, the conservative properties of the model, and hence the accuracy of the results, are best for values close to the Courant criterion. Therefore, the Courant criterion is a valuable index for selecting the time step to be used in the branch-network flow model.

Another equally important consideration in implementation of the branch-network flow model is selection of an appropriate value of the finite-difference weighting factor for the spatial derivatives. Utilizing the weighted, implicit,

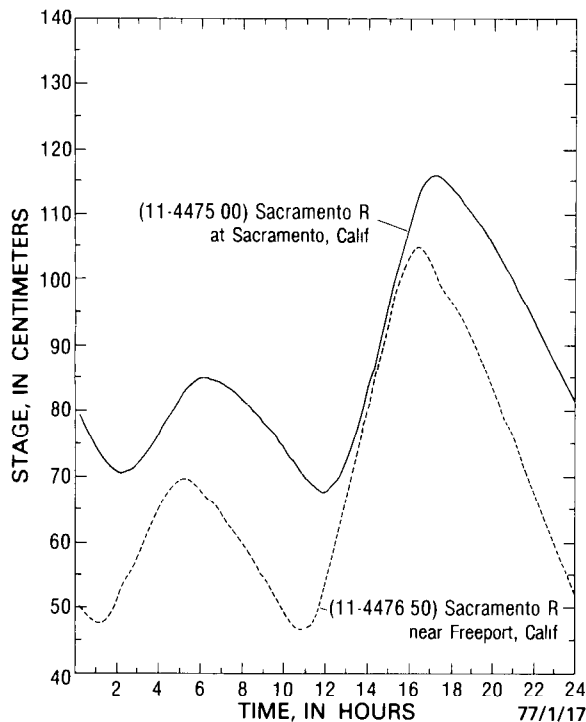


FIGURE 8. — Water-surface elevations for the Sacramento River at Sacramento, Calif., and near Freeport, Calif., used as boundary-value data for the branch-network flow-model simulation shown in figure 7.

four-point difference scheme affords considerable flexibility in simulating various transient-flow conditions. Consequently, it is very important to carefully analyze the flow simulations using various weighting factors for the range of flow conditions expected and to judiciously select the most appropriate value for θ . The effect of the weighting factor on the stability of the solution is illustrated in figure 9. This analysis was accomplished by using the model to simulate perturbed steady flow in the Sacramento River at Sacramento, Calif. In these simulations the stages at Sacramento and near Freeport, used as boundary conditions to drive the model, were fixed at 6.15 m and 4.89 m, respectively, for which the steady flow discharge amounted to 1903.3 m³/s. The initial discharge conditions were set slightly higher at 1903.7 m³/s in order to introduce a perturbation on the flow for conducting the analysis and to illustrate the convergence properties of the model. As figure 9 shows, the model exhibits oscillations in the flow computation for θ values

less than 0.6. These oscillations are small, symmetrical about the true solution, and after their initial development, neither grow nor decay with time. This phenomenon, referred to as pseudoinstability or computational mode, can be negated by taking θ greater than or equal to 0.6, as shown in figure 9. The selection of appropriate values for θ is, however, largely dependent on the particular flow conditions being simulated and the solution time increment. For most transient-flow conditions a reasonable value for the spatial-derivative weighting factor appears to be $0.6 \leq \theta \leq 1.0$. The branch-network flow model defaults to the fully forward scheme specified by θ equal to 1.0; this value of θ produces the most stable computational mode.

Although the direct (noniterative) solution technique in the branch-network flow model produces acceptable results when the selected time step and the chosen schematization are appropriate for the prototype, iteration within the time step is available and can be used to produce results of a higher order accuracy. Such iterative improvement of computed results is optional. Two methods are provided for controlling the iterative refinement process. These controls are intended to be used in tandem. First, the maximum allowable number of iterations can be user specified. Secondly, convergence criteria—the maximum acceptable difference between successive results computed through iteration within the time step—can be specified for both stage and discharge. Default conditions are a maximum of five iterations per time step with the discharge convergence criterion established from the initial values and the stage convergence criterion set at 0.01 ft for data input in the inch-pound system and 1 cm for metric data input. The default discharge convergence criterion is set at one-half of one percent of the minimum (absolute value greater than zero) initial discharge specified. If all initial discharges are zero the discharge convergence criterion is assigned a value of one by default. For the initial convergence test at each new time step the unknowns are automatically set by the model to current time-step values or to model-extrapolated values. The model default is no extrapolation. These parameters provide complete flexibility in controlling the iteration process, thus allowing the model user to tailor

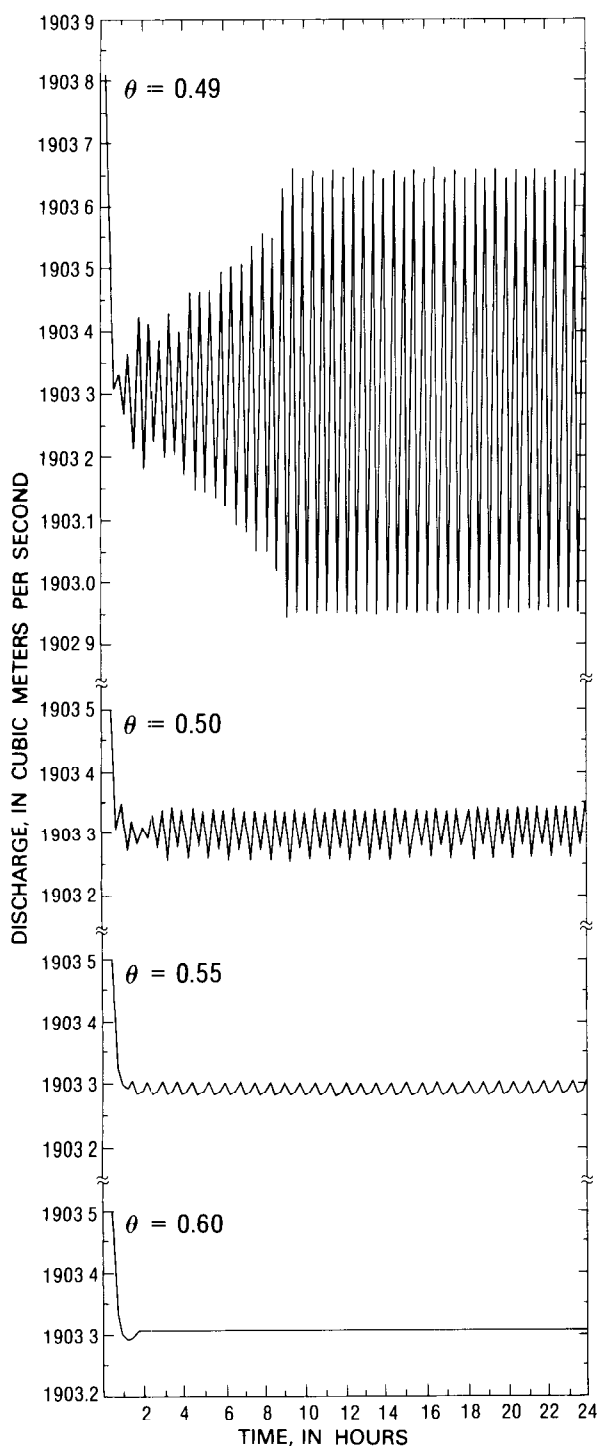


FIGURE 9.—Steady flow computations for the Sacramento River at Sacramento, Calif., by use of various finite-difference weighting factors (θ) in the branch-network flow model.

the computation to suit the accuracy requirements of his particular application. Several applications of the model for various flow conditions have shown that default convergence criteria are generally satisfied in three or less iterations per time step.

Calibration and verification

The success of any flow model application depends greatly on the availability of accurate prototype data. Prototype data are needed for flow-model calibration, that is, determination or refinement of the least quantifiable parameters, such as the flow-resistance coefficient and the water-surface drag coefficient; flow simulations can be properly assessed only through verification with good-quality observed data. In the calibration process the objective is to adjust these parameters to accurately replicate the prototype system for the range of flow conditions expected. Although model reproduction of a prototype water-level hydrograph is of some verification value, a more rigorous verification is achieved by model reproduction of the prototype discharge hydrograph in both phase and amplitude. Once this level of calibration is achieved it is possible to extend the utility of the model to simulate flow conditions beyond the calibration range, if sufficient checks are made to insure the validity of the calibration for such extreme flow conditions.

Data for model calibration and verification consist of time series of measured discharges, together with concurrently recorded water-surface elevations. The length and frequency of required discharge measurements are largely dependent on the unsteady nature of the flow. However, economic and operational constraints often control the duration and frequency of such measurements. In general, for tide-driven systems, one or more measurements, usually of tidal-cycle duration, are scheduled each year. The location of such measurements is based principally on model needs as determined by the prototype flow conditions. Oftentimes, selection of the location at which discharge measurements are to be made is a matter of determining where the flow may be most accurately measured, given the physical and economical constraints on field operations.

All aspects of a particular model schematization are subject to adjustment during the calibration process. However, aspects that are physically well defined and that can be measured, and thus determined with reasonable accuracy, are considerably less subject to adjustments than are those for which measured values are lacking or for which direct determination is impossible. For instance, reach lengths are definable and can be accurately measured; they should not be subject to alteration during calibration. Likewise, channel geometry data are generally not altered during calibration, since such data can be measured with reasonable accuracy. Moreover, water-level boundary-value data, presumably recorded synoptically with precise time synchrony and properly referenced to a common datum, should not require alteration. Yet it is frequently just in this regard that errors occur and model calibration difficulties do arise. Occasionally, one or more water-level recorders may be incorrectly referenced to datum or correctly referenced to an incorrect datum, with the result that not only are the time-sequences of boundary-value data not correct but perhaps the channel geometry may become improperly referenced to stage as well. Recorded boundary-value data that lack time synchrony infer distorted wave-propagation rates within the model and result in phase and amplitude calibration problems. Thus, failure to maintain synchronous operation of the water-level recorders or the presence of errors in the datum reference of these recorders may result in an improperly schematized model and erroneous, often confusing, model results. (One must be particularly sensitive to "force fitting" a model calibration using data of questionable validity.) In order to avoid an unnecessarily complicated and prolonged model-calibration process, it is important to identify and correct errors in the directly measurable quantities as early in the calibration process as possible. It is best, of course, if by thorough planning and diligent field operation, such errors can be avoided entirely.

Once the accuracy of the directly measurable quantities has been verified, the principal aspect of model calibration, namely, determination of the channel conveyance properties, remains to be accomplished. Initially, these properties can

only be approximated, estimated, or otherwise inferred. Thus, the conveyance properties, principally the conveyance due to channel resistance expressed in terms of the Manning equation as

$$K = \frac{1.49}{\eta} AR^{2/3},$$

or, in the metric system, as

$$K = \frac{1}{\eta} AR^{2/3},$$

may legitimately require modification during the calibration. However, the value of the coefficient, η , must always be physically realistic.

Under certain flow conditions the conveyance produced by wind shear acting on the water surface and that resulting from the nonuniform distribution of the flow velocity may also be significant and necessarily require consideration in the calibration process.

The difficulty in evaluating the flow-resistance coefficient for calibrating the flow model stems principally from the fact that the energy-dissipation relationship is an approximation borrowed from the realm of steady, uniform flow. Little factual information is known regarding the effect of boundary-shear resistance under unsteady-flow conditions. Knowledge of the effect of boundary friction is mainly empirical, a fact that complicates model calibration and verification but is not an insurmountable problem. The applicable flow-resistance coefficient is, as noted in the section, Channel conveyance parameters, not only a function of such hydraulic properties as the flow depth, turbulence, and water temperature but also of the schematization of the prototype. Therefore, it is necessary to use the model to arrive at appropriate values, since for different schematizations, different values of η may be found.

In order to conduct the model calibration several accurate sets of discharge data are necessary. It is desirable to have such discharge information for a range of flow conditions. If possible, the model calibration process should begin with a set of data gathered during steady or nearly steady flow conditions. The initial estimate of the flow-resistance coefficient can be determined from the Manning equation or can be simply estimated. The calibration process

then involves successive adjustment of the conveyance factors until satisfactory agreement between the computed and measured flow data is achieved. The model calibration must then be verified by comparative testing with other independent sets of observed-flow data. The model is successfully verified if the computed results agree well with the field-observed data. If agreement is not good, the model calibration parameters must be further adjusted until such agreement is achieved or the cause of the deviation is identified.

By use of the calibrated model of the Sacramento River, several simulations have been conducted to illustrate the effect of changes in the flow-resistance coefficient. In figure 10 the results of these simulations are compared with both measured discharges and with computed discharges from the calibrated model.

A too small value for η reduces flow resistance, thus increasing momentum or inertia. The simulation performed with a decreased flow-resistance coefficient not only results in a discharge hydrograph having peaks and troughs of larger magnitude (fig. 10) but also results in a phase shift, which is not easily discernible in figure 10. On the other hand, an excessive value for η shows the reverse effect. Thus, the model adjustment critically depends on the use of proper η values.

Additional simulations were conducted to illustrate the effects of changes in boundary-value data and cross-sectional geometry. The results of these simulations are compared with both measured discharges and with computed discharges taken from the calibrated model as shown in figures 11 and 12.

Recorded water-surface elevations may sometimes be incorrectly defined because of datum errors, survey inaccuracies, or vertical displacement (settling) of the gaging structure. The result of such errors is an increase or a decrease in the water-surface slope throughout the channel reach. Increasing the water-surface slope increases the discharge in the downstream direction. Reducing the water-surface slope produces the reverse effect, as can be seen from figure 11. To accommodate such detected errors, it is possible, during the flow simulation, to apply a datum correction to the recorded

boundary-value data via an input parameter of the branch-network flow model.

An excessive cross-sectional area, derived by entering a table of stage versus cross-sectional area that represents the schematized channel with too large a value for stage, results in magnification of both positive and negative flows. A too small cross-sectional area, the result of entering a table of stage versus cross-sectional area with too small a value for stage, produces the reverse effect, as can be seen from figure 12. An adjustment to correct the error can be made in the model by using the datum correction input parameter to equally decrease or increase the stage value at the ends of the reach.

Figures 13 and 14 illustrate the computational effects of the weighting factors for the function values and their spatial derivatives in the branch-network flow equations. Selection of appropriate values for these weighting factors is primarily dependent upon the flow conditions and the geometric properties of the prototype. Through use of such variable weighting factors, complete flexibility is provided to accommodate implementation of the model for prototypes having widely varying flow conditions and physical characteristics.

The weighting factor, θ , positions the finite-difference approximation of the spatial derivatives between two adjacent time lines of the space-time grid system. (See fig. 3.) Appropriate values for the spatial derivative weighting factor appear to be in the range $0.6 \leq \theta \leq 1.0$, as noted in the section Computational control parameters. Computational experience has shown that values of θ less than 0.6 have consistently generated unacceptable pseudoinstability (computational mode). The fully forward technique specified by θ equal to 1.0 provides the greatest computational stability. However, it also has the sometimes undesirable characteristic of damping the computed wave. Such numerical damping tends to increase in proportion to increases in the computational time step. Other factors, including the wave celerity, also influence determination of the appropriate θ value. In evaluating θ , an optimal value must be determined so as to minimize numerical damping of the computed transient while at the same time minimizing the

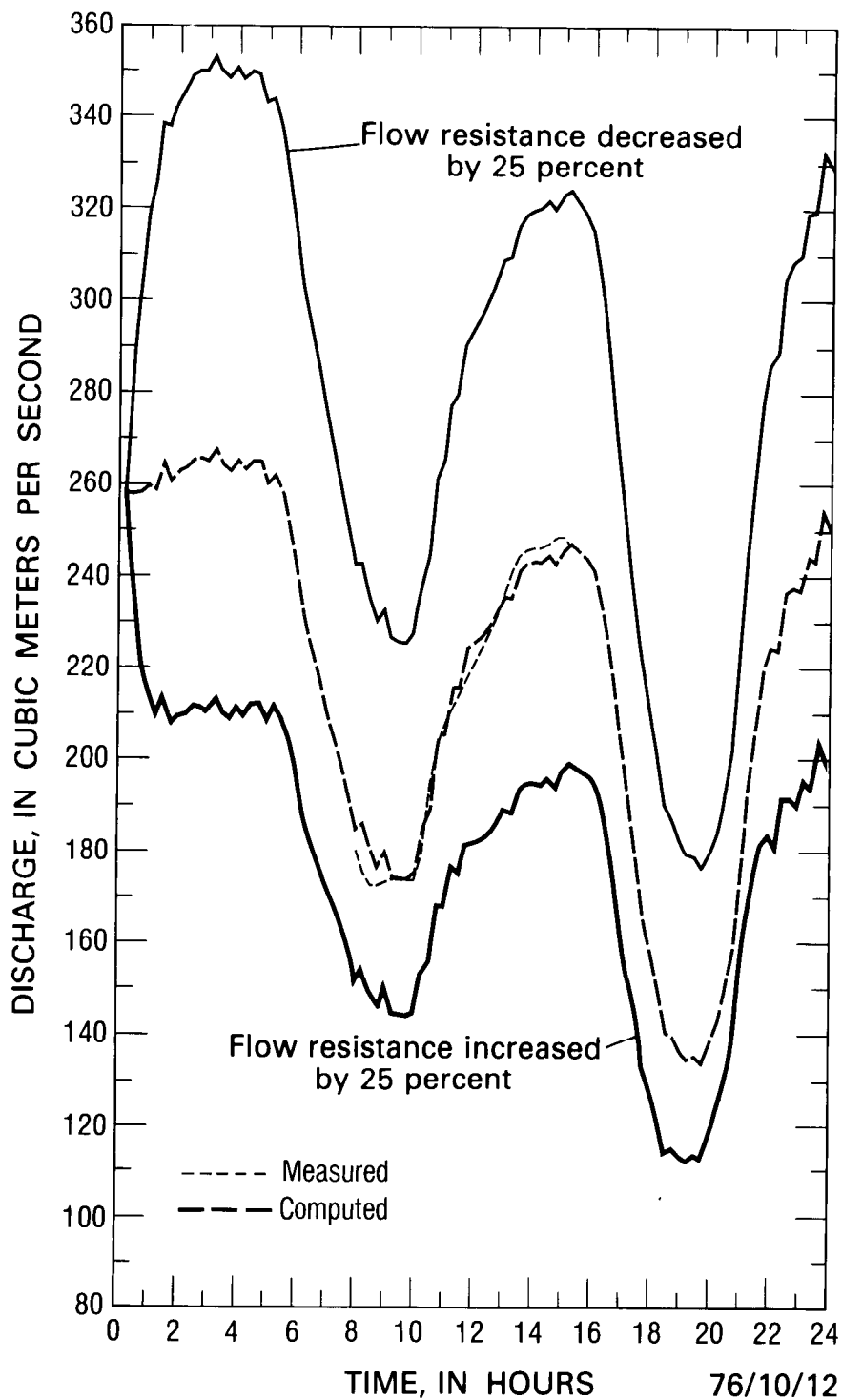


FIGURE 10. — Discharges computed for the Sacramento River at Sacramento, Calif., with flow resistance increased and decreased by 25 percent.

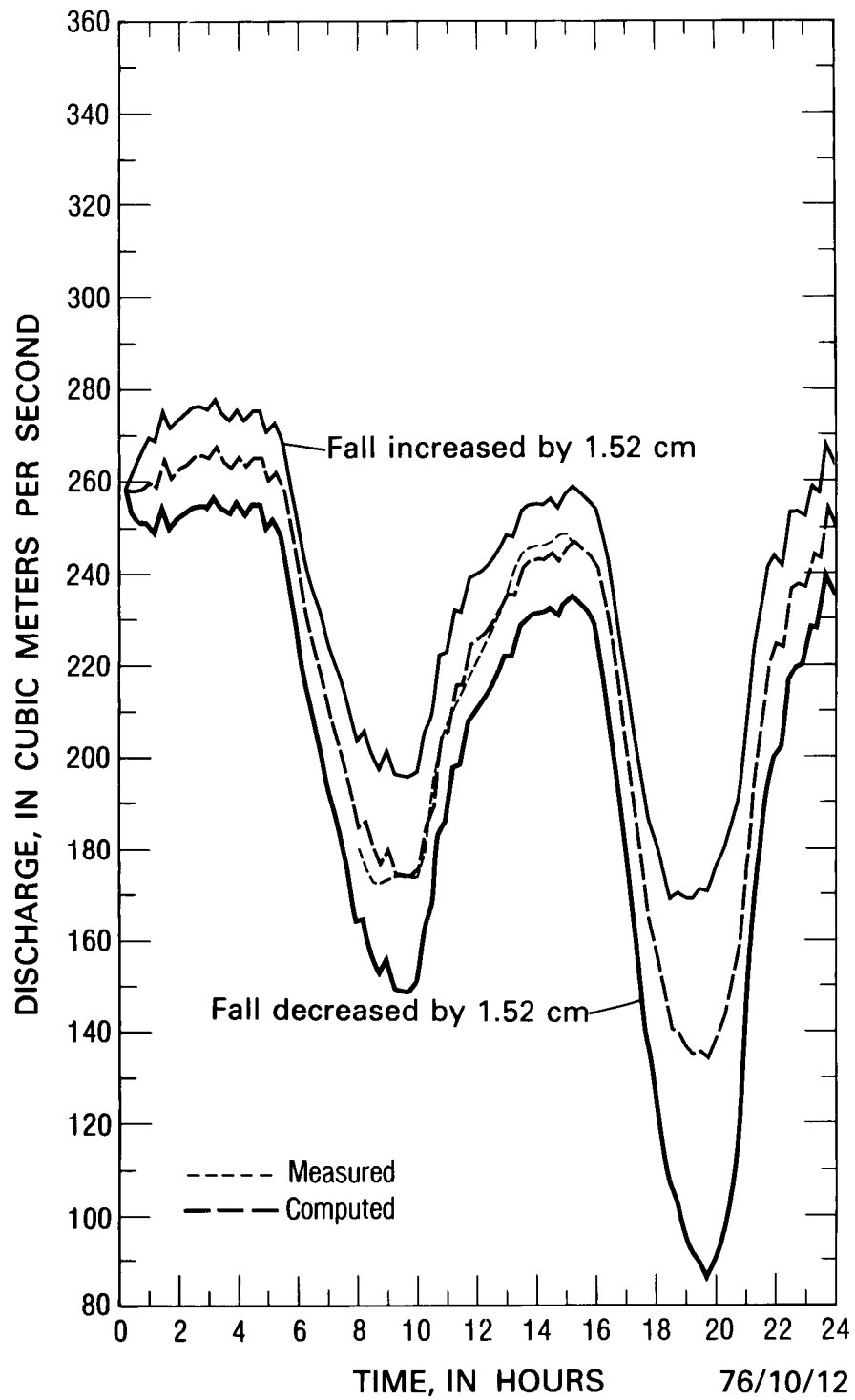


FIGURE 11.—Discharges computed for the Sacramento River at Sacramento, Calif., with the fall increased and decreased by 1.52 cm.

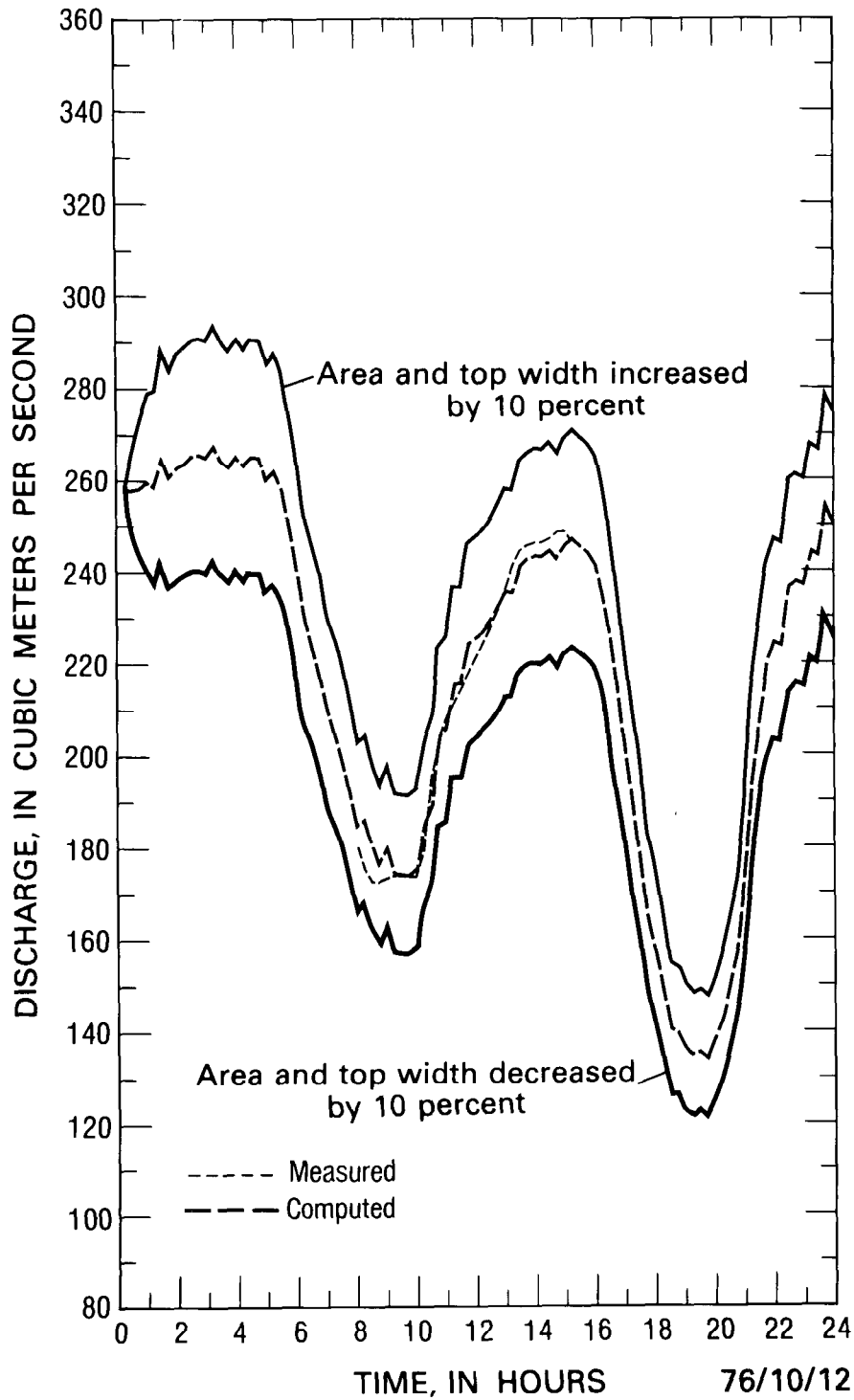


FIGURE 12.—Discharges computed for the Sacramento River at Sacramento, Calif., with the cross-sectional area and top width increased and decreased by 10 per cent.

computational mode, as exemplified in figure 9. Figure 13 indicates a weak pseudoinstability condition manifesting itself in the computed discharge hydrograph for the Sacramento River when a value of 0.6 is used for the spatial-derivative weighting factor. Whereas the discharge hydrograph using a value of 1.0 for θ does not exhibit such pseudoinstabilities, the computed transient is somewhat attenuated, thereby implying a compromise θ value is appropriate for this application.

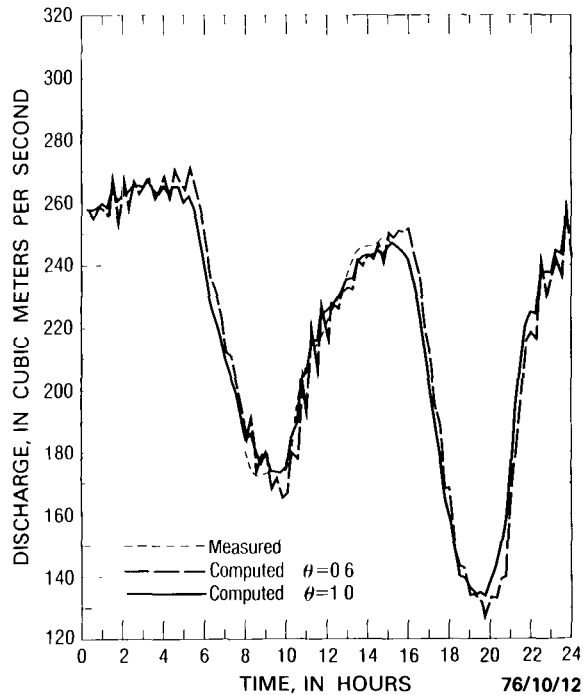


FIGURE 13.—Discharges computed for the Sacramento River at Sacramento, Calif., with various weighting factors (θ) for the spatial derivatives in the branch-network flow model.

In the computation process the geometric properties of area, top width, and hydraulic radius and the discharges in nonderivative form in the equation of motion can be accurately approximated over the time interval by using an appropriate value for the weighting factor, χ . A cursory review of the finite-difference equations for θ and χ , as defined in the section Finite-difference formulation, reveals the similarity between the two weighting factors. Reasonable values for χ fall in the range $0.5 \leq \chi \leq 1.0$. Figure 14 illustrates the effect on the computed

discharges using values of 0.5 and 1.0 for χ . The discharge hydrograph computed using a χ value of 0.5 shows a phase lag compared with that computed using values based totally on the advanced time line, that is, χ equal to 1.0. Subtle differences also exist in the computed minimum discharges. The significance of the weighting factor for these quantities appears to increase for channels having increasingly variable geometric properties, such as, narrowing or widening cross sections. Typically, the weighting factor χ is initially set equal to θ and ultimately adjusted as required during the model calibration process.

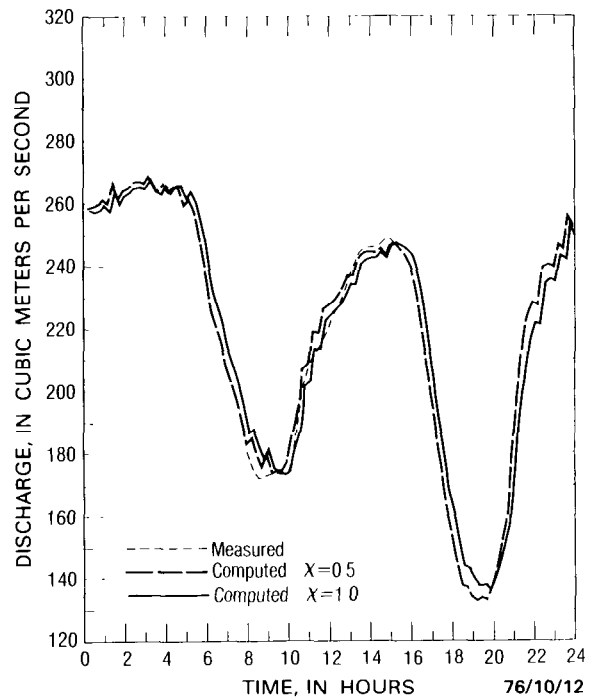


FIGURE 14.—Discharge computed for the Sacramento River at Sacramento, Calif., with various weighting factors (χ) for the function values in the branch-network flow model.

Calibration of network-type flow models may be difficult depending upon the complexity of the flow regime and the interconnection of channels within the prototype. Networks of interconnected open channels generally fall into two categories. In a network of simply connected branches the flow has only one path-of-travel between any two locations in the system. Models of this type of network tend to be easier

to calibrate than models of networks of multiply connected branches, wherein it is possible for the flow to travel by more than one route between various locations. If the calibration of a system of multiply connected branches is not correct, erroneous circulations may appear internally in the network rendering the model results useless. Calibration of network models is best conducted by first subdividing the network into simpler, single- or multiple-branch models keeping intact the principal natural circulation loops of the overall system. After successful calibration of these individual models, evaluation of the complete network model can be undertaken by combining the various smaller subset models. By this technique the network model calibration may be accomplished more systematically and economically.

Branch-Network Program Description

The FORTRAN IV code for the branch-network flow model is listed in Appendix IV. The model is composed of a MAIN program and eight primary subroutines, namely, OUT, PRTPLT, ARBIN, SETA, GEMXPI, OPLOT, DADIO, and DTCODE. The subroutines DADIO and DTCODE, which are referenced by the MAIN program but which are not included in the source listing in Appendix IV, are resident in the time-dependent-data, storage and retrieval system library SCHAF.DADIO-LOADMOD. This library is cataloged on the U.S. Geological Survey computer system. The special system function, MOVE, not identified in the list but used by the MAIN program for fast, efficient array manipulation, is stored in the cataloged FORTRAN library XTENT.LIB. Other lower-level subroutines, aside from the common intrinsic FORTRAN functions, specifically required for the graphical display of computed results and directly referenced via subroutine OPLOT are available in the SYS1.DISSPLA.LIBRARY and SYS1.FLAT-BEDC system program libraries.

For reference purposes and to permit the cross-referencing of program variables and arrays with the mathematical equations, the

MAIN program variables and arrays are defined in Appendix II. Commonality of variable and array names among the MAIN program and the various subroutines has been preserved to the extent practicable.

The bulk of the work of the simulation is performed in the MAIN program module of the model. The primary functions of the MAIN program are numerous:

1. to control the model input and output,
2. to initiate and terminate the simulation,
3. to allocate and appropriately initialize variables and arrays,
4. to retrieve the required boundary-value data and generate the boundary-condition equations,
5. to construct the coefficient matrices and perform the necessary matrix transformations, and
6. to generally supervise the various subprograms and the overall computation process.

The eight primary subroutines of the model perform various functions in support of the simulation conducted by the MAIN program. A matrix solution for the set of branch-transformation equations is effected by Gaussian elimination using maximum pivot strategy in the subroutine GEMXPI. The subroutine SETA computes the flow-resistance coefficient as a linear or quadratic function of water temperature, flow depth, discharge, Froude number, or Reynolds number, as designated by the user according to the prototype flow properties. The ARBIN subroutine interpolates cross-sectional area and top-width properties at a specified stage and approximates the hydraulic radius from the input stage-area-width geometry tables. The subroutine OUT prints computed results in tabular form following each iteration or time step, prints daily summaries of flow results, prints cumulative flow volumes, which it stores and subsequently retrieves from a direct-access file, and optionally punches initial condition cards (for subsequent input to follow-on executions of the model). Line-printer plots of computed results, optionally including plots of measured data, are produced by the PRTPLT subroutine. Similarly, the OPLOT subroutine prepares a daily computed and, optionally, a measured discharge or stage